Electronic Supplementary Information (ESI) for Journal of Materials Chemistry A

A channel-type mesoporous In(III)–carboxylate coordination framework with high physicochemical stability for electrode material of supercapacitor

Miao Du,*[a] Min Chen,[b] Xiao-Gang Yang,[b] Jiong Wen,[b] Xi Wang,[a] Shao-Ming Fang[b] and Chun-Sen Liu*[b]

[a] College of Chemistry, Tianjin Key Laboratory of Structure and Performance for Functional Molecules, MOE Key Laboratory of Inorganic-Organic Hybrid Functional Material Chemistry, Tianjin Normal University, Tianjin 300387, China. E-mail: dumiao@public.tpt.tj.cn

[b] Henan Provincial Key Lab of Surface & Interface Science, Zhengzhou University of Light Industry, Zhengzhou 450002, Henan, China. E-mail: chunsenliu@zzuli.edu.cn

General materials and methods

With the exception of the organic ligand 4,4',4''-(benzene-1,3,5-triyl-tris(oxy))tribenzoic acid (H_3BTTB), which was prepared according to the literature method,[S42] all of the starting reagents and solvents were obtained commercially and used as received. Elemental analysis of C, H, and N was performed on a Vario EL III Elementar analyzer. IR spectrum was measured on a Bruker Tensor 27 OPUS FT-IR spectrometer (KBr pellet) in 4000–400 cm^{-1} range. Powder X-ray diffraction (PXRD) patterns were recorded on a Bruker D8 Advance diffractometer (Cu-Kα, λ = 1.5406 Å) at 40 kV and 100 mA, and the intensity data were recorded by continuous scans in a $2\theta/\theta$ mode with a scan speed of 2 s/step and a step size of 0.02°. Simulation of the PXRD patterns was performed by the single-crystal data and diffraction-crystal module of the *Mercury* (Hg) program. Thermogravimetric analysis (TGA) experiments were carried out on a Perkin-Elmer Diamond SII thermal analyzer (from 25 to 800 °C) with a heating rate of 5 °C min^{-1} under nitrogen atmosphere. The morphologies of 437-MOF samples with different treatments were characterized by using a JEOL-JSM-7001F field-emission scanning electron microscope (SEM) at an acceleration voltage of 10 kV.

The gas sorption isotherms were collected on a Micromeritics 3Flex surface area and pore size analyzer under ultrahigh vacuum in a clean system, with a diaphragm and turbo pumping system. Ultrahigh-purity-grade (> 99.999%) N_2, Ar, O_2, CO_2, and He gases were applied in all adsorption measurements. The experimental temperatures were maintained by liquid nitrogen (77 K), liquid argon (87 K), and dry ice-acetone baths (195 K).

X-ray data collection and structure determination

Single-crystal X-ray diffraction data for 437-MOF, 437-MOF-CH_2Cl_2 (after solvent-exchange with CH_2Cl_2 for three times), and 437-MOF-boiling water (after treatment in boiling water for one hour) were collected on an Oxford Xcalibur Gemini Eos diffractometer by using graphite-monochromated Cu-Kα radiation (λ = 1.54178 Å) at 294(2) K. Multi-scan absorption corrections were performed with the *CrysAlisPro* program.[S43] Empirical absorption corrections were carried out using spherical harmonics, implemented in *SCALE3 ABSPACK* scaling algorithm. The final structures were solved by direct methods, and all non-H atoms were refined

anisotropically by full-matrix least-squares method with the SHELXTL software package.[S44] H atoms of the hydroxyl anions were located in the difference maps and then allowed to ride on the parent atoms for refinements [with $U_{iso}(H) = 1.2U_{eq}(O)$]. H atoms of benzene ring were located in calculated sites and treated in the subsequent refinement as riding atoms [C–H = 0.93 Å and $U_{iso}(H) = 1.2U_{eq}(C)$]. Attempts to locate and model the highly disordered solvent molecules (H_2O, NMF, or CH_2Cl_2 molecules) in the pores were unsuccessful. Therefore, the SQUEEZE routine, a part of the PLATON package of crystallographic software[S45] was used to calculate the solvent disorder area and remove the diffraction contribution from these solvents to give a set of solvent free diffraction intensity. Crystal data and structural refinement details for 437-MOF, 437-MOF-CH_2Cl_2, and 437-MOF-boiling water were listed in Table S3. A comparison of the selected bond parameters was given in Table S4.

Formula determination of 437-MOF

According to the result of single crystal X-ray determination, the framework of 437-MOF can be formulated as $\{[In(BTTB)_{2/3}(OH)](solvent)\}_n$ with $Z = 6$ in the unit cell. As the highly disorder guest solvents cannot be determined by the current X-ray diffraction data, the identification of these included molecules was further taken by elemental analysis and thermogravimetric analysis (TGA). The TGA curve (see Fig. S1) of 437-MOF indicates that the exclusion of solvent molecules occurs in the temperature range of 25–180 °C, with no further weight loss up to ca. 400 °C. After that, the host framework will be destroyed with ligand decomposition upon heating. Since 437-MOF was prepared in NMF solvent, the excluded solvent molecules should be NMF and/or H_2O (coming from the starting reagents). Also, according to the result of elemental analyses (observed: C, 40.69%; H, 5.23%; N, 8.50%), the formula of 437-MOF can be determined as $\{[In(BTTB)_{2/3}(OH)](NMF)_5(H_2O)_4\}_n$ in which the C, H, and N contents (calculated: 40.94%, 5.40%, 8.53%) are well consistent with the observed values. In addition, the observed weight loss of solvents (44.65%) in TGA curve also agrees well with the calculated value (44.73%), which further confirms this formula.

Calculation of BET surface area of 437-MOF samples

BET equation: $$V = \frac{CVmx}{(1-x)[1+(c-1)x]}$$

where $x = P/P_0$, V is the volume of gas adsorbed per gram of sample at standard temperature and pressure (STP), Vm is the monolayer capacity, and C is related to the heat of adsorption.

The equation can be rewritten in the form:

$$\frac{P}{V(P_0 - P)} = \frac{1}{VmC} + \frac{C-1}{VmC} \times \frac{P}{P_0}$$

The BET analysis was performed by plotting $P/[V(P_0 - P)]$ vs. P/P_0. The slope ($[C - 1]/VmC$) and y intercept ($1/VmC$) of this linear region give the monolayer capacity. Vm is used to calculate the surface area from $A = \mathrm{Vm}\sigma_0 N_{\mathrm{AV}}$, in which σ_0 is the cross-sectional area of the adsorbate at solid or liquid density (16.2 Å^2 for N_2). Two major criteria were established to aid the choice of pressure range for the BET analysis:[S94] (1) The pressure range selected should have values of $V(P_0 - P)$ increasing with P/P_0. (2) The y intercept of the linear region must be positive to yield a meaningful value of the C parameter, which should be greater than zero. A BET surface area was obtained by using the data points on the sorption branch of N_2 isotherm at 77 K in the Micromeritics 3Flex 1.01.01 software package.

Pore size distribution of MOFs

Pore size distribution (PSD) data for all 437-MOF samples were determined by analyzing the N_2 isotherms at 77 K using the non-local density functional theory (DFT) and implementing a hybrid kernel based on a zeolite/silica model containing the cylindrical pores, as implemented in the 3Flex 1.01.01 software package.

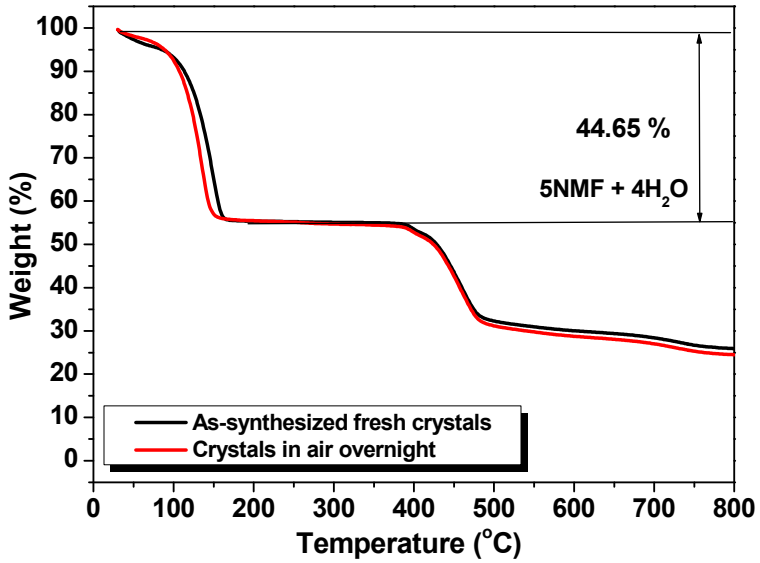

Fig. S1 TGA curves of 437-MOF: (black curve) as-synthesized fresh crystal sample and (red curve) crystal sample placed in air overnight.

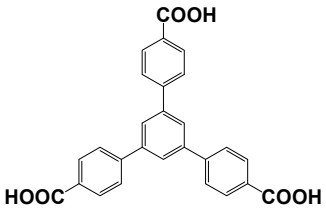

4,4',4"-benzene-1,3,5-triyl-tribenzoic acid
(H_3BTB)

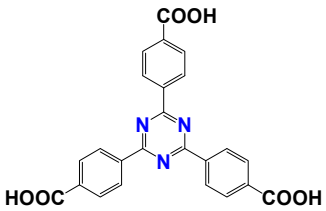

4,4',4"-*s*-triazine-2,4,6-triyl-tribenzoic acid
(H_3TATB)

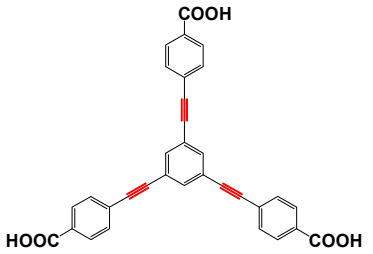

4,4',4"-[benzene-1,3,5-triyl-tris(ethyne-2,1-diyl)]tribenzoic acid
(H_3BTE)

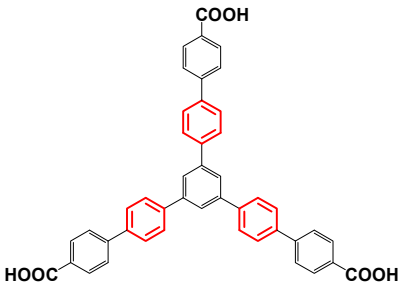

4,4',4"-(benzene-1,3,5-triyl-tris(benzene-4,1-diyl))tribenzoic acid
(H_3BBC)

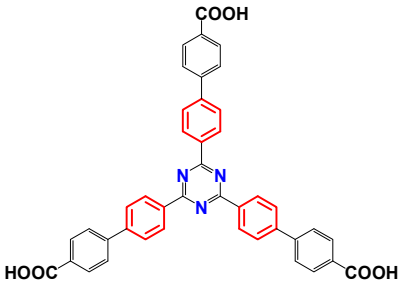

4,4',4"-(triazine-2,4,6-triyl-tris(benzene-4,1-diyl))tribenzoic acid
(H_3TAPB)

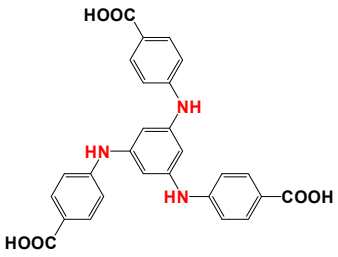

4,4',4"-(benzene-1,3,5-triyl-tris(azanediyl))tribenzoic acid)
(H_3BTATB)

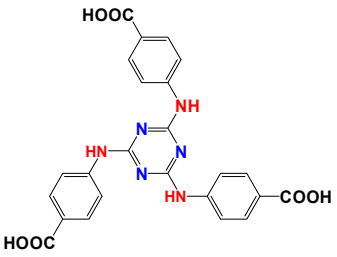

4,4',4"-*s*-triazine-1,3,5-triyl-tri-*p*-aminobenzoic acid
(H_3TATAB)

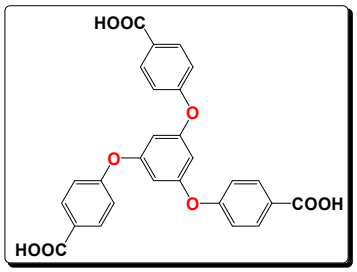

4,4',4"-(benzene-1,3,5-triyl-tris(oxy))tribenzoic acid
(H_3BTTB)

Scheme S1 Selected trigonal carboxylic ligands derived from trimesic acid.

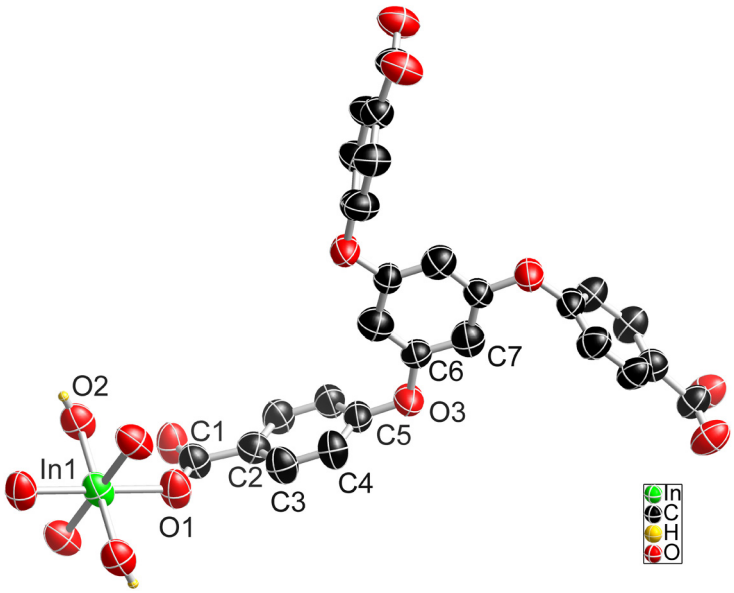

Fig. S2 A fragment of 437-MOF with the ellipsoids drawn at the 50% probability level.

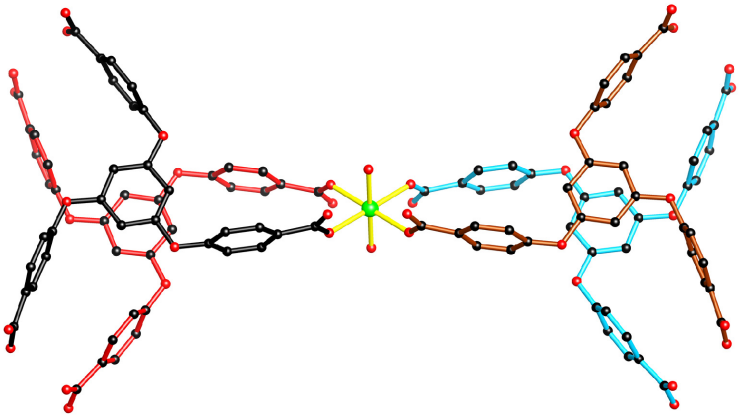

Fig. S3 View of the local coordination geometry of In(III) in 437-MOF. The BTTB ligands are distinguished by different colors for clarity.

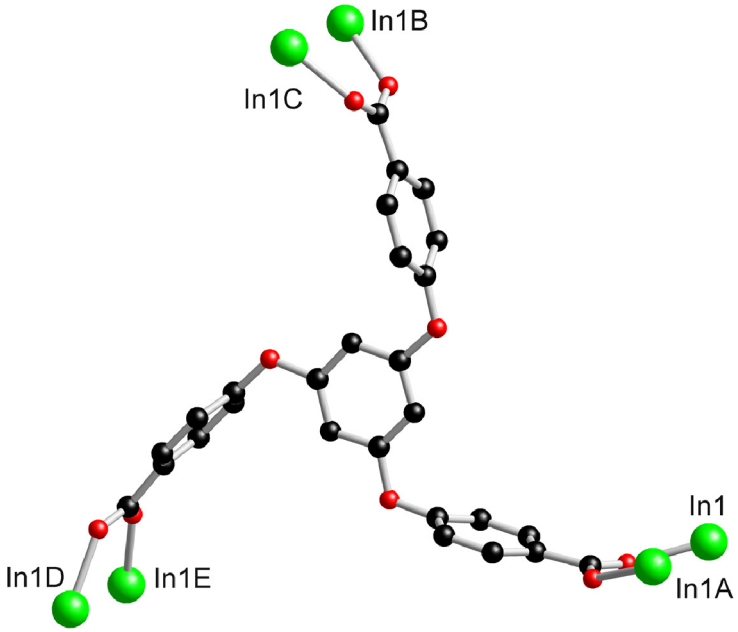

Fig. S4 Coordination mode of the BTTB ligand (A = –*x* + 1, –*y* + 2, *z* + 1/2; B = –*y* + 1, *x* – *y* + 1, *z*; C = *y* – 1, –*x* + *y*, *z* + 1/2; D = *x* – *y* + 1, *x*, *z* + 1/2, and E = –*x* + *y*, –*x* + 1, *z*).

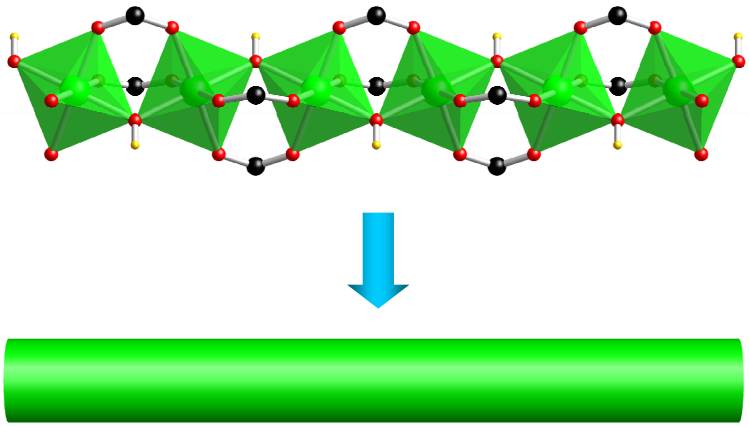

Fig. S5 View of the 1-D rod-shaped SBU.

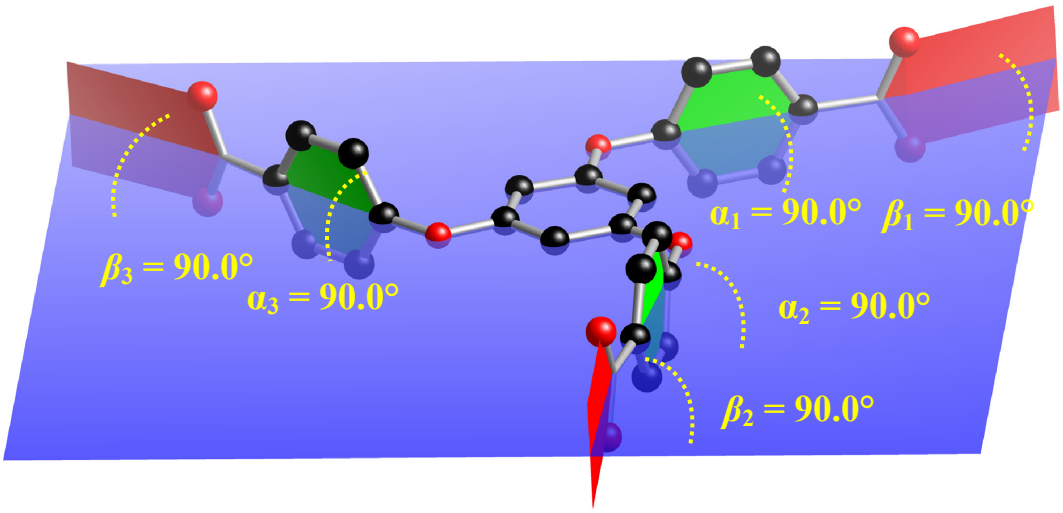

Fig. S6 View of the perpendicular arrangement between the benzene core and the three benzene arms or the attached carboxylates (α is the dihedral angle between benzene arms and benzene core; β is the dihedral angle between carboxylate groups and benzene core).

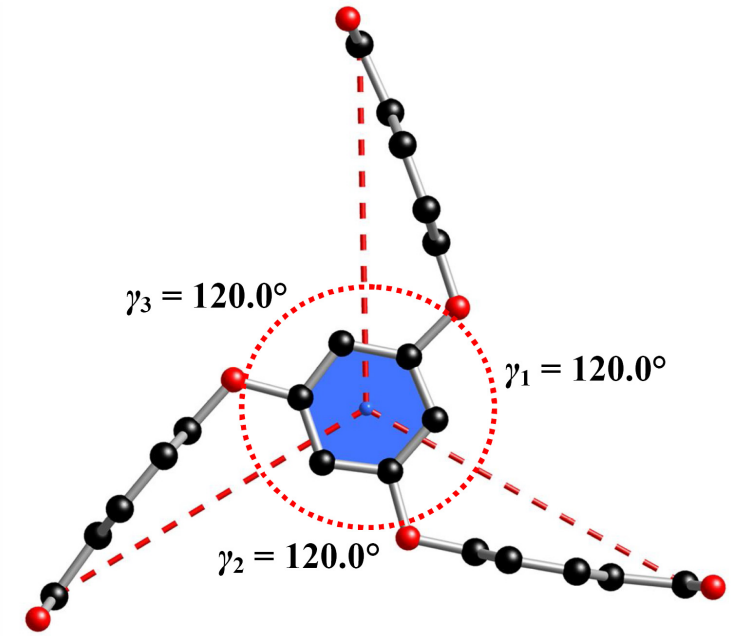

Fig. S7 View of the equilateral triangle constituted by three carboxylate carbon atoms, the centroid of which is just the center of benzene core (γ is the obtuse angle between two adjacent lines linked by the center of benzene core and the carboxylate carbon atom).

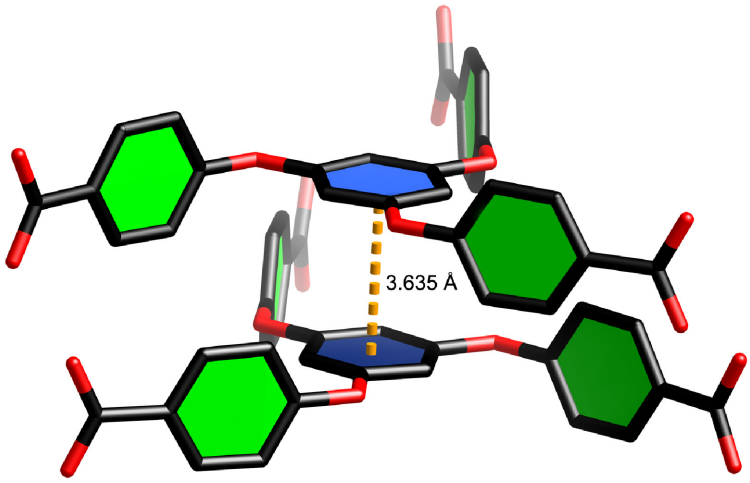

Fig. S8 Strong π···π stacking interaction between two parallel benzene cores.

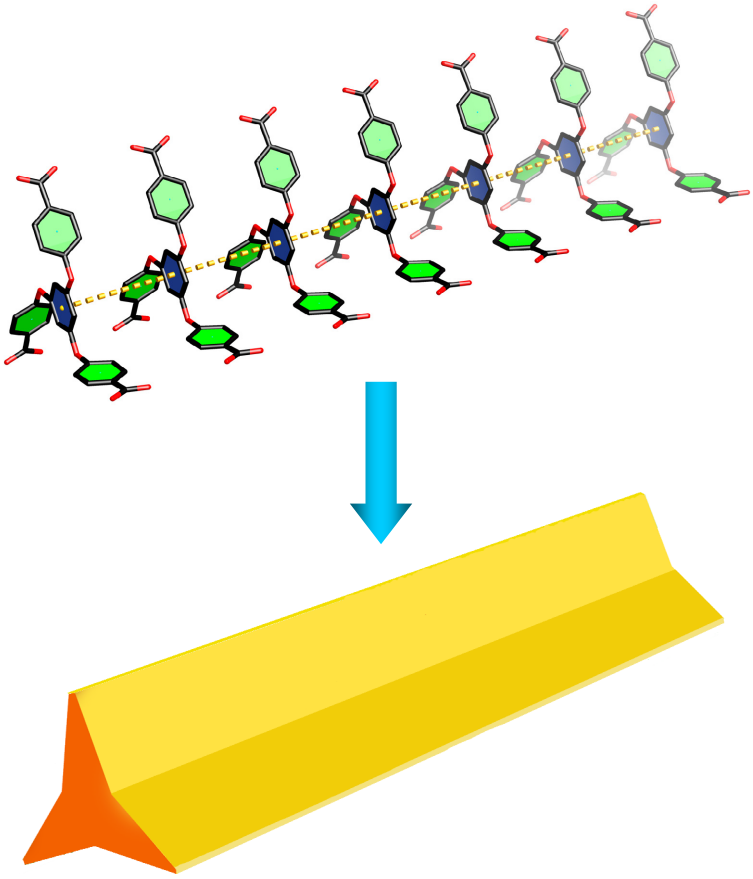

Fig. S9 (top) Stick and (bottom) schematic views of the 1-D organic supramolecular array.

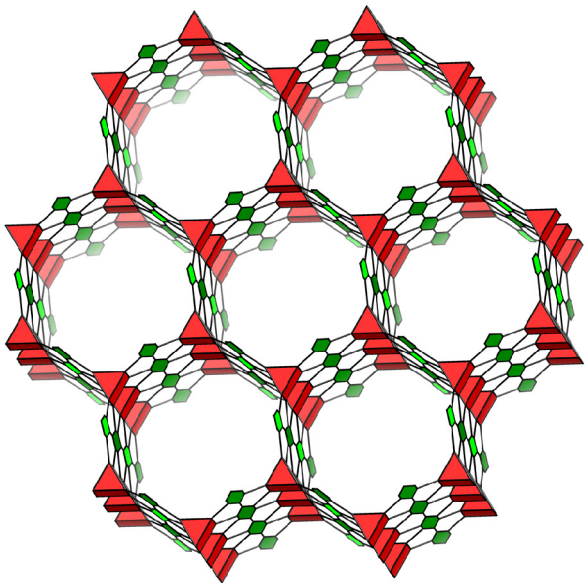

Fig. S10 The augmented version of two-nodal six-connected 3-D network of 437-MOF. (BTTB and metal nodes are shown by triangular prism and hexagon, respectively).

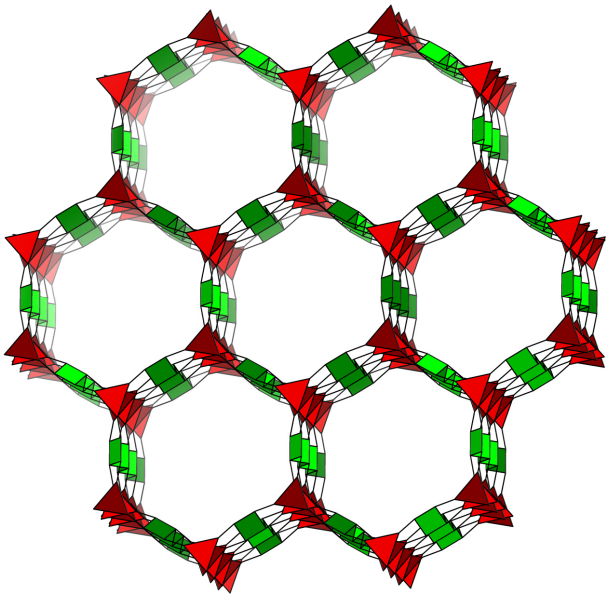

Fig. S11 Schematic representation of the (3,4)-connected topological network of 437-MOF, according to the concept of infinite rod-shaped SBUs.

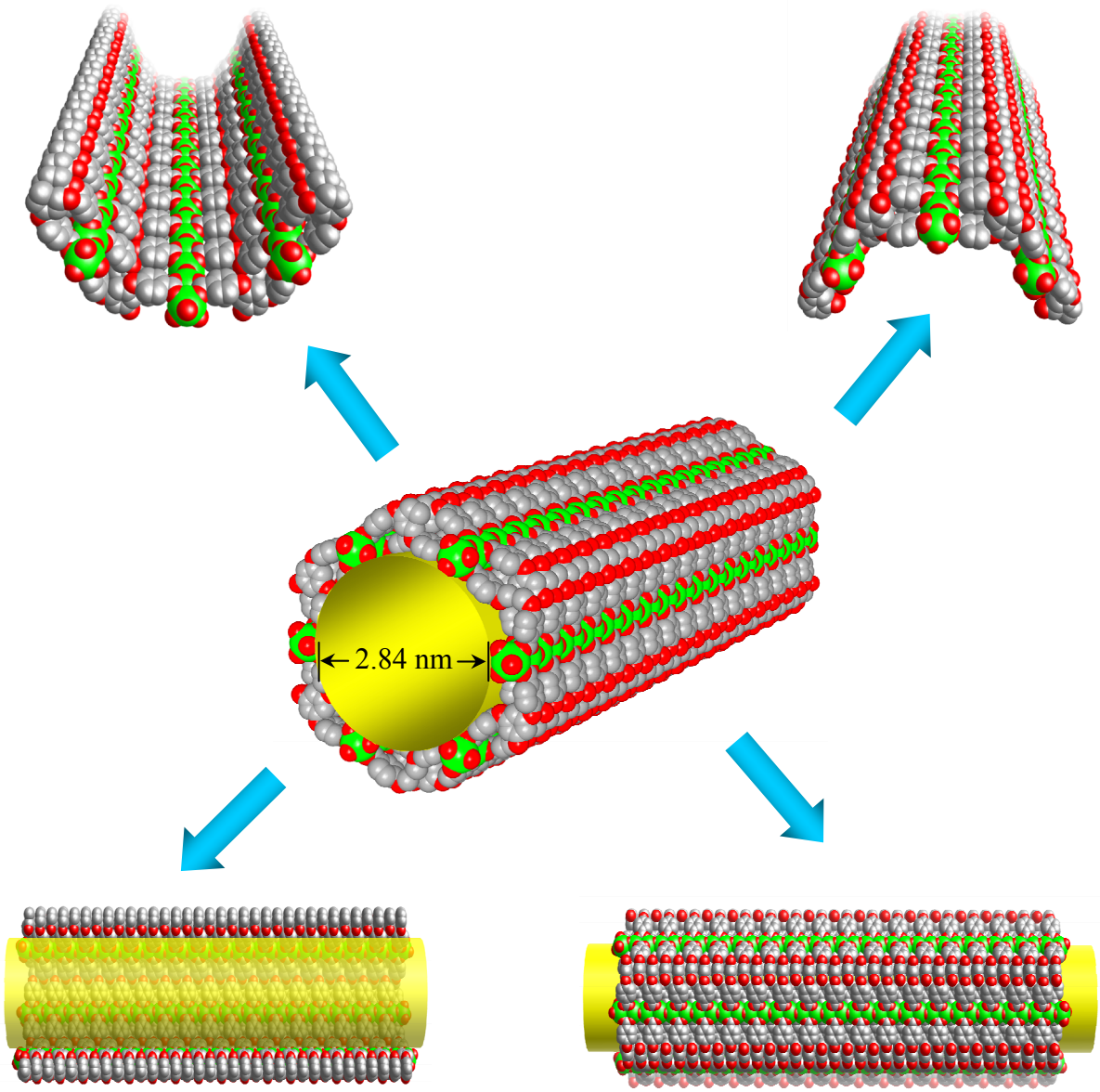

Fig. S12 Hybrid nanotube-like structure of 437-MOF viewed from different sides (Carbon: grey, Oxygen: red, and Indium: green).

Physicochemical stability of 437-MOF

Thermal stability of 437-MOF. The as-synthesized sample (ca. 10 mg) was placed inside a pre-weighed 12-mm quartz sample tube and then evacuated upon heating under different conditions for PXRD measurement (see Fig. S13). The final product, upon a long-term heating at 400 °C in vacuum, can be properly indexed to cubic In_2O_3 (JCPDS No. 65-3170).

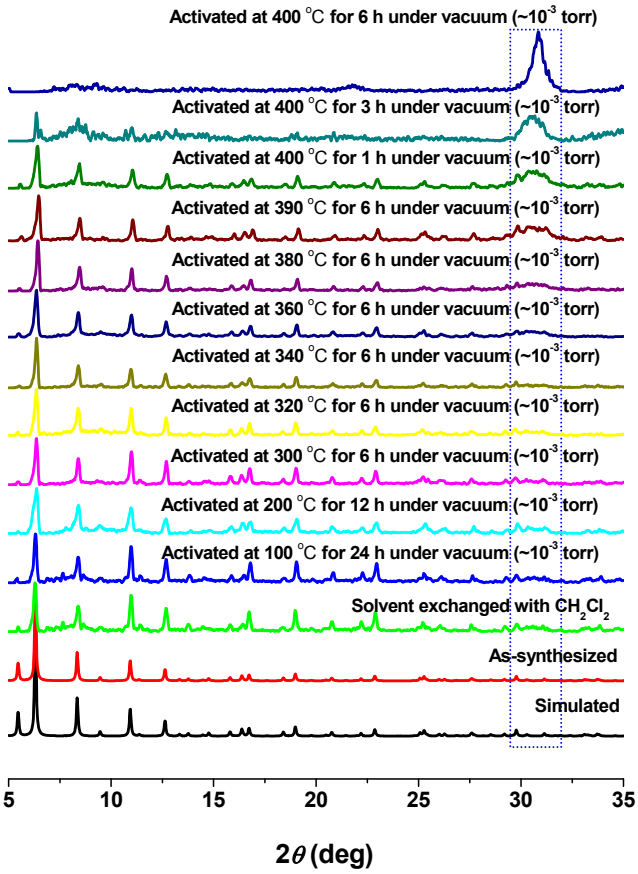

Fig. S13 PXRD patterns for heat-resistance investigation of 437-MOF.

Chemical stability of 437-MOF. The as-synthesized sample (ca. 30 mg) was suspended in 15 mL water and left at room temperature. After immersion, the sample was filtered and dried in air at room temperature for PXRD measurement (see Fig. S14).

The as-synthesized sample (ca. 30 mg) was dispersed into 30 mL water in a vial and then sealed into a Teflon-lined stainless steel vessel, which was heated at 100 °C in an oven. After heating, the sample was cooled down, filtered, and dried in air at room temperature for PXRD measurement (see Fig. S15).

The as-synthesized sample (ca. 10 mg) was suspended in 5 mL common organic solvent, H_2O_2 (30%, aq.), HCl water solution, or NaOH water solution, at ambient temperature for at least 12 hours. Then, the sample was filtered and dried in air at room temperature for PXRD measurement (see Fig. S16 and Fig. S17).

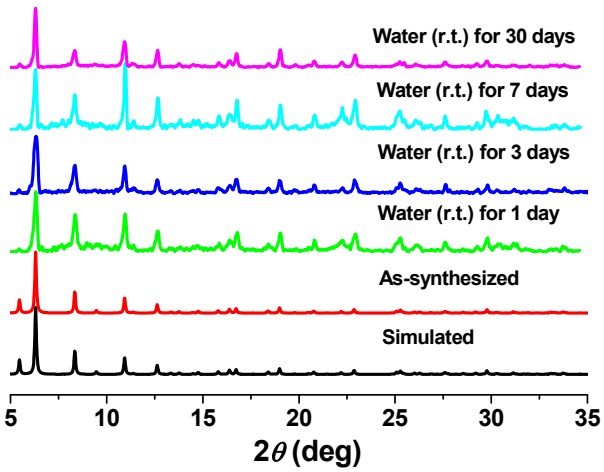

Fig. S14 PXRD patterns of 437-MOF via treating in water at room temperature for various durations from 1 day to 30 days.

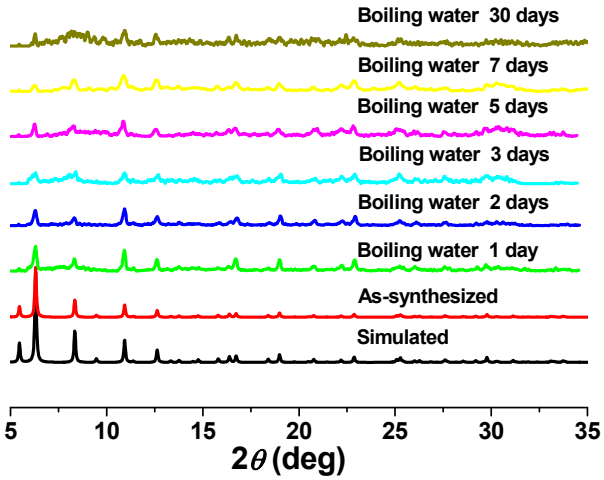

Fig. S15 PXRD patterns of 437-MOF via treating in water at 100 °C for various durations from 1 day to 30 days.

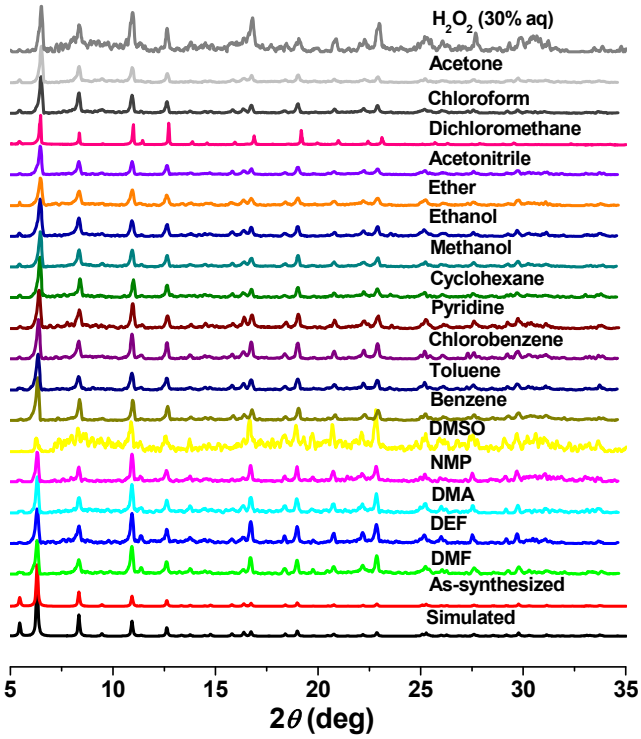

Fig. S16 PXRD patterns of 437-MOF via treating in common organic solvents and hydrogen peroxide (aq. 30%) overnight.

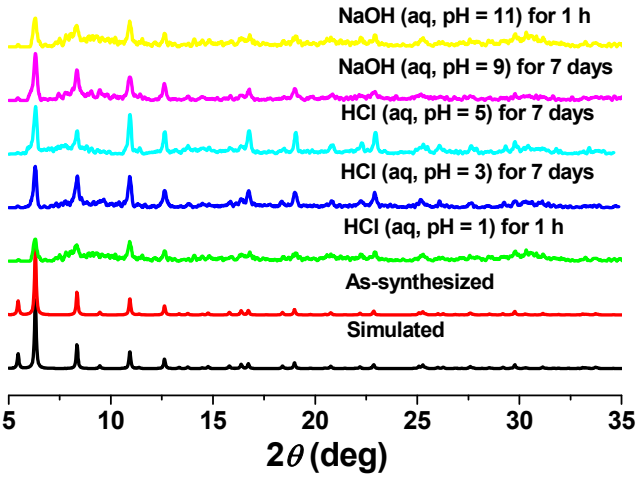

Fig. S17 PXRD patterns of 437-MOF via treating in HCl and NaOH water solutions of pH = 1, 3, 5, 9, and 11 for various durations from 1 hour to 7 days.

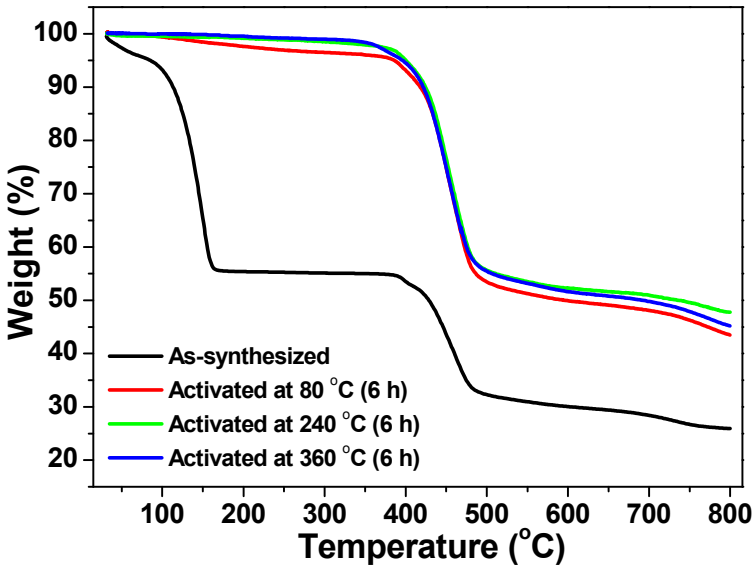

(a)

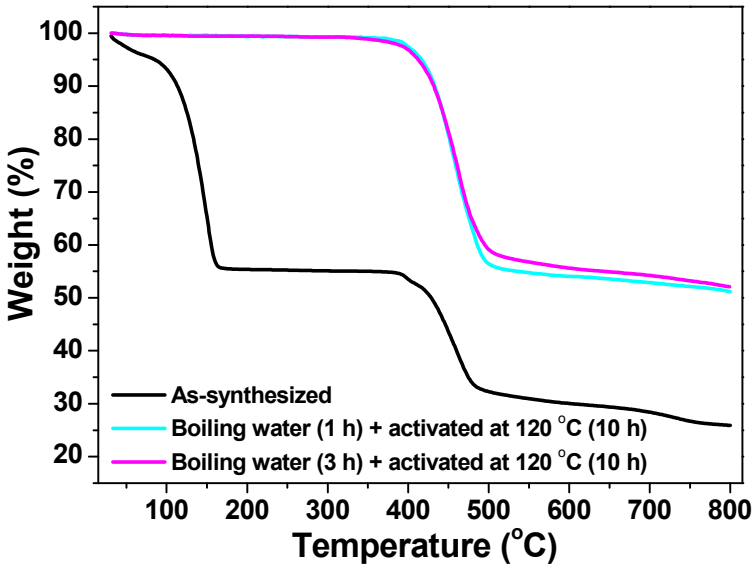

(b)

Fig. S18 TGA curves of (a) the as-synthesized 437-MOF, 437-MOF-80, 437-MOF-240, and 437-MOF-360, and (b) the as-synthesized 437-MOF, 437-MOF-boiling water, and 437-MOF-boiling water-3h.

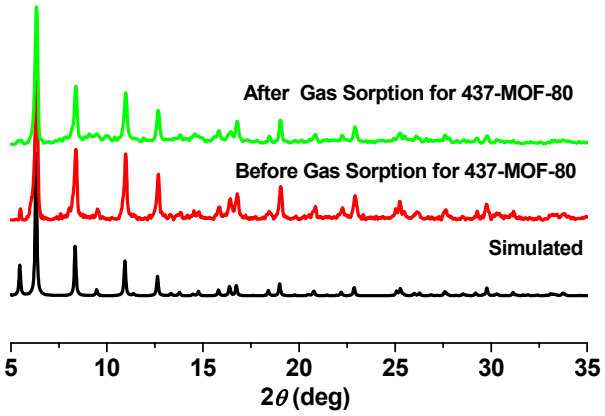

Fig. S19 PXRD patterns of 437-MOF-80 before and after gas sorption.

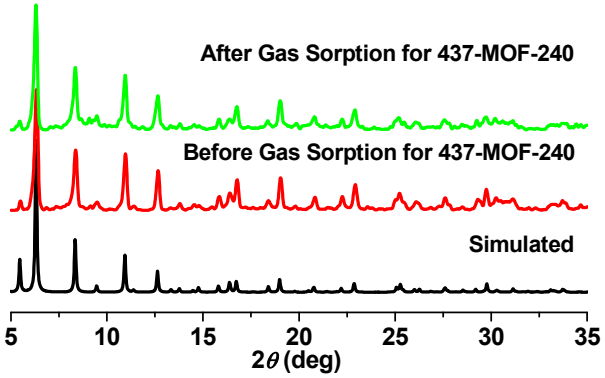

Fig. S20 PXRD patterns of 437-MOF-240 before and after gas sorption.

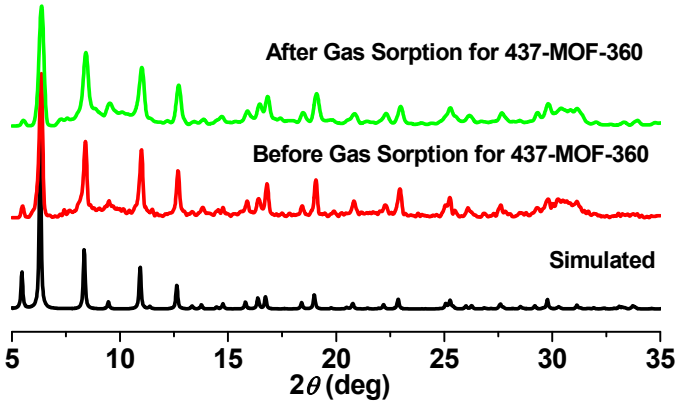

Fig. S21 PXRD patterns of 437-MOF-360 before and after gas sorption.

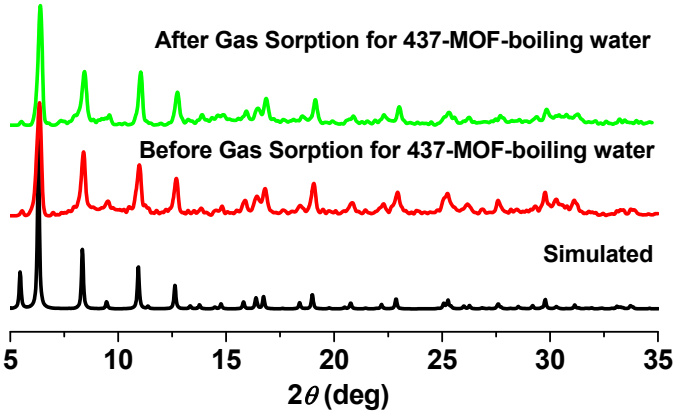

Fig. S22 PXRD patterns of 437-MOF-boiling water before and after gas sorption.

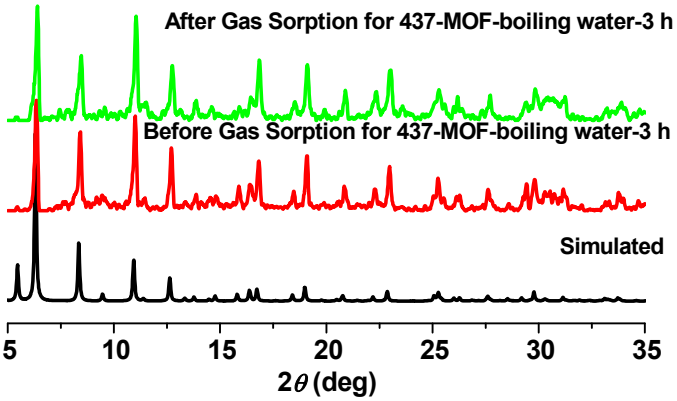

Fig. S23 PXRD patterns of 437-MOF-boiling water-3h before and after gas sorption.

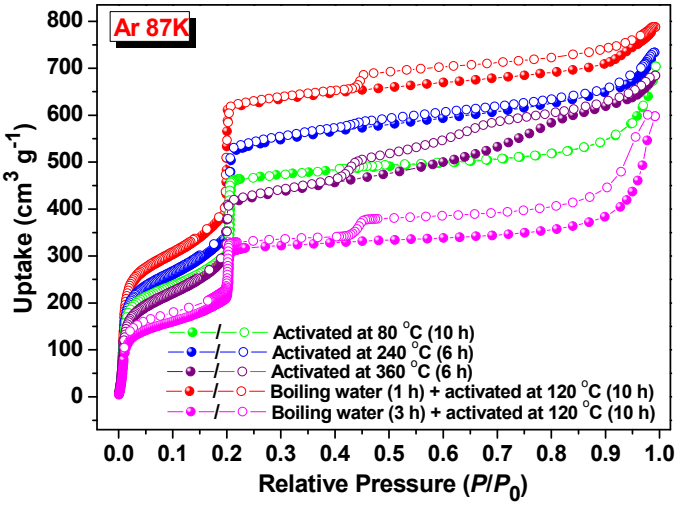

Fig. S24 Ar sorption isotherms at 87 K for 437-MOFs activated at different conditions (filled/open circles: adsorption/desorption).

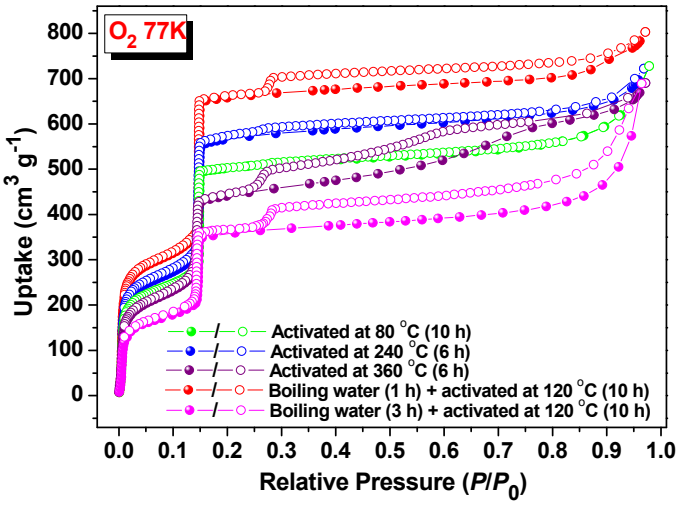

Fig. S25 O_2 sorption isotherms at 77 K for 437-MOFs activated at different conditions (filled/open circles: adsorption/desorption).

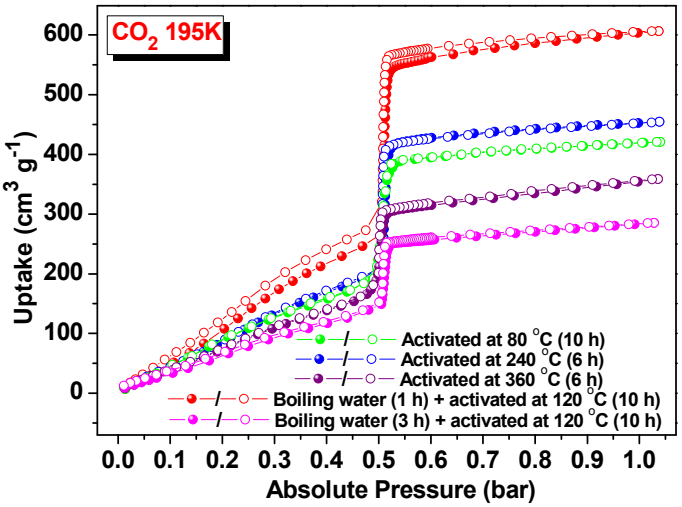

Fig. S26 CO_2 sorption isotherms at 195 K for 437-MOFs activated at different conditions (filled/open circles: adsorption/desorption).

Vapor adsorption analyses of 437-MOF

The sorption isotherms of H_2O and C_6H_6 in vapor state were measured for 437-MOF-80 with Micromeritics 3Flex surface area and pore size analyzer. The temperature was maintained by temperature-programmed water bath (298 K). The adsorption isotherm of water indicates only surface sorption on the material (Fig. S27), while C_6H_6 vapor can be gradually adsorbed onto the sample in the lower pressure. The C_6H_6 uptake will increase as the vapor pressure raises. The adsorption features of H_2O and C_6H_6 should be attributed to hydrophobization of the pore walls for 1-D channels in 437-MOF.

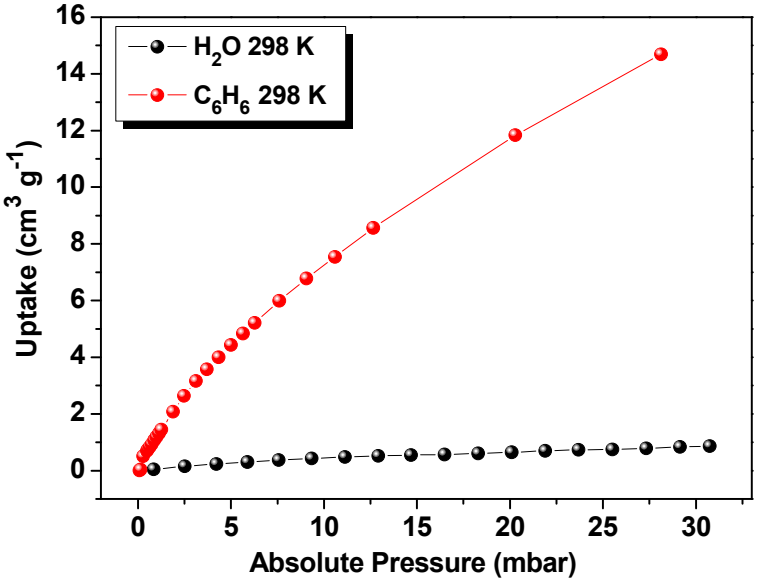

Fig. S27 H_2O and C_6H_6 adsorption isotherms of 437-MOF-80.

Table S1 The structural features of reported mesoMOFs.

Publish Time	*meso*MOF Code	*meso*MOF Formula[a]	Structural Type	Cavity-/ Channel-diameters (Å)[b]	SBUs and/or SBBs	Topology symbol[c]	Ref.
2004	MIL-100	$[Cr_3F(H_2O)_3O(\mathbf{BTC})_2](H_2O)_n$ ($n \approx 28$)	Cage	25.0 × 25.0 29.0 × 29.0	Cr_3O, Super tetrahedron	MTN	S1
2005 2006	MIL-101	$[Cr_3F(H_2O)_2O(\mathbf{BDC})_3](H_2O)_n$ ($n \approx 25$)	Cage	29.0 × 29.0 34.0 × 34.0	Cr_3O, Super tetrahedron	MTN	S2 S3
2007	N.A.[d]	$[Tb_{16}(\mathbf{TATB})_{16}(DMA)_{24}](DMA)_{91}(H_2O)_{108}$	Cage	39.1 × 39.1 47.1 × 47.1	Tb_4 cluster, Truncated super tetrahedron	dia	S4
2008	N.A.[d]	$[Cu_6O(\mathbf{TZI})_3(H_2O)_9(NO_3)](H_2O)_{15}$	Cage	15.9 × 15.9 22.0 × 22.6 23.3 × 23.3	Paddle-wheel, $Cu_3O(N_4CR)_3$, Truncated cuboctahedron	rht	S5
2008	ZIF-95	$[Zn(\mathbf{CBIM})_2]$	Cage	25.1 × 14.3 30.1 × 20.0	N.A.[d]	poz	S6
	ZIF-100	$[Zn_{20}(\mathbf{CBIM})_{39}(OH)]$		35.6 × 35.6	N.A.[d]	moz	
2009	UMCM-2	$[Zn_4O(\mathbf{T^2DC})(\mathbf{BTB})_{4/3}]$	Cage	14.0 × 17.0 23.9 × 23.9 26.0 × 32.0	Zn_4O	N.A.[d]	S7
2009	PCN-61	$[Cu_3(\mathbf{BTEI})(H_2O)_3](DMF)_5(H_2O)_4$	Cage	13.0 × 13.0 15.0 × 15.0	Paddle-wheel, Cuboctahedron	N.A.[d]	S8
	PCN-66	$[Cu_3(\mathbf{NTEI})(H_2O)_3](DMA)_{21}(H_2O)_{10}$		23.0 × 23.0 13.0 × 13.0 16.0 × 16.0 26.0 × 26.0	Paddle-wheel, Cuboctahedron	N.A.[d]	

Table S1 (*continued*)

Publish Time	*meso*MOF Code	*meso*MOF Formula[a]	Structural Type	Cavity-/ Channel-diameters (Å)[b]	SBUs and/or SBBs	Topology symbol[c]	Ref.
2009	MIL-101-NDC	$[Cr_3(OH)(H_2O)_2(\mu_3\text{-}O)(2,6\text{-}\mathbf{NDC})_3](guest)$ (guest = H_2O, EtOH)	Cage	39.0 × 39.0 46.0 × 46.0	Cr_3O, Super tetrahedron	MTN	S9
2009	NOTT-112	$[Cu_3(\mathbf{L^1})(H_2O)_3](DMSO)_8(DMF)_{15}(H_2O)_3$	Cage	13.0 × 13.0 13.9 × 13.9 20.0 × 20.0	Paddle-wheel	N.A.[d]	S10
2009	DUT-6	$[Zn_4O(2,6\text{-}\mathbf{NDC})(\mathbf{BTB})_{4/3}](DEF)_{16}(H_2O)_{9/2}$	Cage	25.0 × 25.0 30.0 × 30.0	Zn_4O	pto	S11
2010	MOF-180	$[Zn_4O(\mathbf{BTE})_2](DMF)_{14.8}(NMP)_{15.6}$	Cage	15.0 × 23.0	Zn_4O	qom	S12
	MOF-200	$[Zn_4O(\mathbf{BBC})_2(H_2O)_3](DEF)_{29.4}(NMP)_{32.2}$		18.0 × 28.0	Zn_4O	qom	
	MOF-210	$[Zn_4O(\mathbf{BTE})_{4/3}(\mathbf{BPDC})](DMF)_{25.7}(NMP)_{24.6}$		26.9 × 48.3	Zn_4O	toz	
2010	NOTT-116	$[Cu_3(\mathbf{PTEI})(H_2O)_3](DMF)_{16}(H_2O)_{26}$	Cage	12.0 × 12.0[e] 14.8 × 14.8[e] 23.2 × 23.2[e]	Paddle-wheel, Cuboctahedra	rht	S13
2010	PCN-68	$[Cu_3(\mathbf{PTEI})(H_2O)_3](DMF)_{33}(H_2O)_{13}$					S14
2010	PCN-610	$[Cu_3(\mathbf{TTEI})(H_2O)_3](DMF)_{22}(H_2O)_{19}$[e]	Cage	12.0 × 12.0[e] 18.6 × 18.6[e] 26.0 × 26.0[e]	Paddle-wheel, Cuboctahedra	rht	S14
2010	NU-100						S15
2010	PCN-100	$[Zn_4O(\mathbf{TATAB})_2](DEF)_{17}(H_2O)_3$	Cage	27.3 × 27.3 27.3 × 27.3	Zn_4O	pyr	S16
	PCN-101	$[Zn_4O(\mathbf{BTATB})_2](DEF)_{16}(H_2O)_5$					
2010	N.A.[d]	$[(In_3O)(OH)(\mathbf{ADC})_2(\mathbf{IN})_2](H_2O)_{4.67}$	Cage	9.5 × 33.9	$In_3O(O_2CR)_6X_3$	$(3^2.4^{17}.5^7.6^2)$	S17
2011	JT-1	$[\{Cu_7(OH)_2(\mathbf{L^2})_3\}\{Cu_6(OH)_2(SO_4)_3(S_3O_{10})_2\}](H_2O)_{10}$	Cage	23.6 × 23.6	Cu_6, Cu_7 cluster	N.A.[d]	S18
	JT-2	$[\{Cu_7(OH)_2(\mathbf{L^2})_3\}_2\{Cu_6(OH)_2(SO_4)_6(S_2O_7)\}$ $\{Cu_3(SO_4)(H_2O)_6\}](H_2O)_{18}$		18.0 × 18.0 23.0 × 23.0	Cu_6, Cu_7 cluster	N.A.[d]	

Table S1 (*continued*)

Publish Time	*meso*MOF Code	*meso*MOF Formula[a]	Structural Type	Cavity-/ Channel-diameters (Å)[b]	SBUs and/or SBBs	Topology symbol[c]	Ref.
2011	PCN-69	$[Cu_3(\mathbf{BTTI})(H_2O)_3](DMF)_{20}(H_2O)_{16}$	Cage	13.0 × 13.0[f] 24.1 × 24.1[f] 25.0 × 25.0[f]	Paddle-wheel, Cuboctahedra	ubt	S19
2011	NOTT-119	$[Cu_3(\mathbf{BTTI})(H_2O)_3](DMF)_{35}(H_2O)_{35}$					S20
2011	N.A.[d]	$[Zn_4O(\mathbf{L^3})_{1.5}]$ $[Zn_4O(\mathbf{L^4})_{1.5}]$ $[Zn_4O(\mathbf{L^5})_{1.5}]$	Cage	31.0 × 31.0 37.4 × 37.4 38.4 × 38.4	$Zn_4O(CO_2)_6$	cor	S21
2012	PCN-53	$[Fe_3O(H_2O)_3(\mathbf{BTTC})_2](DMF)_{10}$	Cage	12.5 × 12.5 14.8 × 14.8 22.2 × 22.2	$[Fe_3O(O_2CR)_6]$	$(4^2.6)_2$ $(4^4.6^4.8^6.10)$	S22
2012	PCN-105	$[Cd_4Na(H_2O)_2(\mathbf{HTDBD})_3(\mathbf{TDBD})](DMF)_{10}(EtOH)_6(H_2O)_3$	Cage	20.0 × 20.0 21.0 × 21.0	Pentanuclear	reo	S23
2012	DUT-25	$[Zn_4O(\mathbf{BENZTB})(\mathbf{BTB})_{2/3}](DEF)_{16}(H_2O)_{7/2}$	Cage	8.0 × 18.0 20.0 × 32.0	$[Zn_4O(CO_2)_6]$	nbo	S24
2012	SUMOF-1-Zn	$[Zn_6(\mathbf{BTB})_4(4,4'\text{-}\mathbf{bpy})_3](solvent)_x$	Cage	21.0 × 21.0	Paddle-wheel	pto	S25
	SUMOF-1-Co	$[Co_6(\mathbf{BTB})_4(4,4'\text{-}\mathbf{bpy})_3](solvent)_x$		21.0 × 21.0	Paddle-wheel	pto	
2012	N.A.[d]	$[Cu_3(\mathbf{L^6})]$ $[Cu_3(\mathbf{L^7})]$	Cage	12.0 × 12.0 15.0 × 15.0 23.0 × 23.0 12.0 × 12.0 15.0 × 15.0 23.0 × 23.0	Paddle-wheel	N.A.[d]	S26
2013	MIL-143	$[Fe_3O(Cl^-)(H_2O)_2(\mathbf{BDC})_{3/2}(\mathbf{BTB})](solvent)_n$	Cage	20.0 × 20.0 24.0 × 24.0	Super tetrahedra	reo	S27
2013	N.A.[d]	$[(CH_3)_2NH_2]_2[Zn(\mathbf{TATAT})_{2/3}](DMF)_3(H_2O)$	Cage	21.0 × 21.0	N.A.[d]	N.A.[d]	S28

Table S1 (*continued*)

Publish Time	*meso*MOF Code	*meso*MOF Formula[a]	Structural Type	Cavity-/ Channel-diameters (Å)[b]	SBUs and/or SBBs	Topology symbol[c]	Ref.
2002	**IRMOF-16**	$[Zn_4O(\mathbf{TPDC})_3](DEF)_{17}(H_2O)_2$	3D Channel	28.8 × 28.8	Zn_4O	pcu	S29
	IRMOF-14	$[Zn_4O(\mathbf{PDC})_3](DEF)_6(H_2O)_5$		24.5 × 24.5			
	IRMOF-12	$[Zn_4O(\mathbf{HPDC})_3](DEF)_{10}(H_2O)$		24.5 × 24.5			
	IRMOF-10	$[Zn_4O(\mathbf{BPDC})_3](DEF)_{12}(H_2O)$		24.5 × 24.5			
	IRMOF-8	$[Zn_4O(2,6\text{-}\mathbf{NDC})_3](DEF)_6$		21.4 × 21.4			
2006	**MesoMOF-1**	$[Cu_3(\mathbf{TATAB})_2(H_2O)_3](DMF)_8(H_2O)_9$	3D Channel	22.5 × 26.1	Paddle-wheel, Cuboctahedra	bor	S30
2009	**N.A.**[d]	$[Cu_2(\mathbf{L^8})(H_2O)_2](DMF)_{14}(H_2O)_5$	3D Channel	3.5 × 21.2	$[Cu_2(O_2CR)_4]$	pts	S31
2010	**CMOF-2a**	$[(R\text{–}\mathbf{L^{9a}})Cu_2(H_2O)_2](DMF)_{15}(H_2O)_{11}$	3D Channel	22.0 × 15.0 11.0 × 11.0	Paddle-wheel	$(4^3.6^2.8)$	S32
	CMOF-3a	$[(R\text{–}\mathbf{L^{10a}})Cu_2(H_2O)_2](DEF)_{12}(H_2O)_{16}$		30.0 × 20.0 14.0 × 14.0			
	CMOF-4a	$[(R\text{–}\mathbf{L^{11a}})Cu_2(H_2O)_2](DEF)_{10}(DMA)_{14}(H_2O)_5$		32.0 × 24.0 19.0 × 19.0			
	CMOF-2b	$[(R\text{–}\mathbf{L^{9b}})Cu_2(H_2O)_2](DEF)_{11}(H_2O)_3$		22.0 × 15.0 13.0 × 13.0			
	CMOF-3b	$[(R\text{-}\mathbf{L^{10b}})Cu_2(H_2O)_2](DMF)_{13}(^i PrOH)_{11}(H_2O)_{4.5}$		30.0 × 20.0 16.0 × 16.0			
	CMOF-4b	$[(R\text{–}\mathbf{L^{11b}})Cu_2(H_2O)_2](DEF)_{6.5}(DMF)_{19}(^i PrOH)_{8.5}(H_2O)_2$		32.0 × 24.0 21.0 × 21.0			
2010	**CMOF-2**	$[Zn_4(\mu_4\text{-}O)(\mathbf{L^{12}})_3](DEF)_{22}(H_2O)_4$	3D Channel	26.0 × 26.0	Paddle-wheel	pcu	S33
	CMOF-3	$[Zn_4(\mu_4\text{-}O)(\mathbf{L^{13}})_3](DMF)_{42}$		20.0 × 20.0			
	CMOF-4	$[Zn_4(\mu_4\text{-}O)(\mathbf{L^{13}})_3](DEF)_{37}(EtOH)_{23}(H_2O)_4$		32.0 × 32.0			
2010	**Cd-MOF**	$[Cd(\mathbf{NH_2BDC})(4,4'\text{-}\mathbf{bpy})](DMF)_3(H_2O)_{4.5}$	3D Channel	18.0 × 23.0	**N.A.**[d]	kag	S34

Table S1 (*continued*)

Publish Time	*meso*MOF Code	*meso*MOF Formula[a]	Structural Type	Cavity-/ Channel-diameters (Å)[b]	SBUs and/or SBBs	Topology symbol[c]	Ref.
2012	PCN-222(Fe)	N.A.[d]	3D Channel	9.2 × 11.0 37.0 × 37.0	Zr_6 cluster	kag	S35
2012	Bio-MOF-100	$[(CH_3)_2NH_2]_4[Zn_8(\mathbf{AD})_4(\mathbf{BPDC})_6O_2](DMF)_{49}(H_2O)_{31}$	3D Channel	28.0 × 28.0	Zinc-adeninate octahedra	lcs	S36
2013	N.A.[d]	$[(CH_3)_2NH_2]_2[ZnNa_2(\mu_2\text{-}H_2O)_2(H_2O)_2(\mathbf{TATAT})](DMF)_2$	3D Channel	17.0 × 23.0	Rod-shaped chain	pts-x	S28
2013	Bio-MOF-101 Bio-MOF-102 Bio-MOF-103	$[(CH_3)_2NH_2]_2[Zn_8(\mathbf{AD})_4(2,6\text{-}\mathbf{NDC})_6(OH)_2](DMF)_{34}(H_2O)_{13.4}$ $[(CH_3)_2NH_2]_2[Zn_8(\mathbf{AD})_4(\mathbf{ABDC})_6(OH)_2]$ $[(CH_3)_2NH_2]_2[Zn_8(\mathbf{AD})_4(\mathbf{NH_2\text{-}TPDC})_6(OH)_2]$	3D Channel	21.0 × 21.0 28.0 × 28.0 29.0 × 29.0	Zinc-adeninate octahedra	lcs	S37
2008	UMCM-1	$Zn_4O(\mathbf{BDC})(\mathbf{BTB})_{4/3}$	Microcage + 1D Channel	14.0 × 17.0 27.0 × 32.0	Zn_4O	N.A.[d]	S38
2013	CYCU-3	$[Al(OH)(\mathbf{SDC})]$	Multiple 1D Channel	14.4 × 14.4 28.3 × 31.1	Rod-shaped chain	N.A.[d]	S39
2007	JUC-48	$[Cd_3(\mathbf{BPDC})_3(DMF)](DMF)_5(H_2O)_{18}$	1D Channel	24.5 × 27.9	Rod-shaped chain	etb	S40
2012	IRMOF-74-III IRMOF-74-IV IRMOF-74-V IRMOF-74-VI IRMOF-74-VII IRMOF-74-IX IRMOF-74-XI	N.A.[d]	1D Channel	22.2 × 27.3 28.0 × 32.8 35.2 × 41.1 41.1 × 49.1 49.4 × 57.5 60.5 × 71.8 84.5 × 98.1	Rod-shaped chain	etb	S41
	437-MOF	$\mathbf{[In(BTTB)_{2/3}(OH)](NMF)_5(H_2O)_4}$	**1D Channel**	**32.3 × 32.3**	**Concave triangular prism**	$(3^3.4^6.5^6)_2(3^4.4^4.5^4.6^3)_3$	**This work**

[a] Abbreviations:
BTC = benzene-1,3,5-tricarboxylate;
BDC = benzene-1,4-dicarboxylate;
TATB = 4,4',4''-*s*-trizaine-2,4,6-triyltribenzoate;
TZI = 5-tetrazolylisophthalate;
CBIM = 5-chlorobenzimidazolate;
T^2DC = thieno[3,2-b]thiophene-2,5-dicarboxylate;
BTB = 4,4',4''-benzene-1,3,5-triyl-tribenzoate;
BTEI = 5,5',5''-benzene-1,3,5-triyltris(1-ethynyl-2-isophthalate);
NTEI = 5,5',5''-(4,4',4''-nitrilotris(benzene-4,1-diyl)tris(ethyne-2,1-diyl))triisophthalate;
2,6-**NDC** = 2,6-naphthalenedicarboxylate;
L^1 = 1,3,5-tris(3',5'-dicarboxy[1,1'-biphenyl]-4-yl)benzene;
BTE = 4,4',4''-[benzene-1,3,5-triyl-tris(ethyne-2,1-diyl)]tribenzoate;
BBC = 4,4',4''-(benzene-1,3,5-triyl-tris(benzene-4,1-diyl))tribenzoate;
BPDC = 4,4'-biphenyldicarboxylate;
PTEI = 5,5'-((5'-(4-((3,5-dicarboxyphenyl)ethynyl)phenyl)-[1,1':3',1''-terphenyl]-4,4''-diyl)-bis(ethyne-2,1-diyl))diisophthalate;
TTEI = 5,5',5''-(((benzene-1,3,5-triyltris(ethyne-2,1-diyl))tris(benzene-4,1-diyl))tris-(ethyne-2,1-diyl))triisophthalate;
TATAB = 4,4',4''-*s*-triazine-1,3,5-triyltri-*p*-aminobenzoate;
BTATB = 4,4',4''-(benzene-1,3,5-triyltris(azanediyl))tribenzoate;
ADC = azobenzene-4,4'-dicarboxylate;
IN = isonicotinate;
L^2 = (*R*)-*N,N'*-Bis(3-*tert*-butyl-5-(4-pyridyl)salicylidene)-3,3'-diamino-5,5',6,6'-tetramethyl-2,2'-methoxymethyl-1,1'-biphenyl;
BTTI = 5,5',5''-(benzene-1,3,5-triyl-tris(biphenyl-4,4'-diyl))triisophthalate;
L^3 = 4,4'-(2,2-bis((4-carboxy-2-methoxyphenoxy)methyl)propane-1,3-diyl)bis(oxy)bis(3-methoxybenzoate);
L^4 = 3,3'-(4,4'-(2,2-bis((4-(2-carboxyvinyl)-2-methoxyphenoxy)methyl)propane-1,3-diyl)bis(oxy)bis(3-methoxy-4,1-phenylene))diacrylate;
L^5 = 6,6'-(2,2-bis((6-carboxynaphthalen-2-yloxy)methyl)propane-1,3-diyl)bis(oxy)di-2-naphthoate;
BTTC = benzo-(1,2;3,4;5,6)-tris(thiophene-2'-carboxylate);
H_2HTDBD = 4,4'-(6-hydroxy-1,3,5-triazine-2,4-diyl)bis(azanediyl)dibenzoic acid;
BENZTB = *N,N,N',N'*-benzidinetetrabenzoate;
4,4'-**bpy** = 4,4'-bipyridine;
L^6 = *N,N',N''*-tris(isophthalyl)-4,4',4''-benzene-1,3,5-triyl-tribenzamide;
L^7 = *N,N',N''*-tris(isophthalyl)-4,4',4''-*s*-triazine-2,4,6-triyl-tribenzamide;

TATAT = 5,5',5"-(1,3,5-triazine-2,4,6-triyl)tris(azanediyl)triisophthalate;
TPDC = *p*-terphenyl-4,4"-dicarboxylate;
PDC = 2,7-pyrenedicarboxylate;
HPDC = 2,7-tetrahydropyrenedicarboxylate;
$\mathbf{L^{8}}$ = methanetetra(biphenyl-*p*-carboxylate);
$\mathbf{L^{9a}}$ = (*R*)-(2*E*,2'*E*,2"*E*,2'"*E*)-3,3',3",3'"-(2,2'-diethoxy-1,1'-binaphthyl-4,4',6,6'-tetrayl)tetraacrylate;
$\mathbf{L^{10a}}$ = (*R*)-2,2'-diethyoxy-1,1'-binaphthyl-4,4',6,6'-tetrakis(4-benzoate);
$\mathbf{L^{11a}}$ = *(R)*-4,4',4",4'"-(1*E*,1'*E*,1"*E*,1'"*E*)-2,2',2",2'"-(2,2'-diethoxy-1,1'-binaphthyl-4,4',6,6'-tetrayl)tetrakis(ethene-2,1-diyl)tetrabenzoate;
$\mathbf{L^{9b}}$ =*(R)*-(2*E*,2'*E*,2"*E*,2'"*E*)-3,3',3",3'"-(2,2'-dihydroxy-1,1'-binaphthyl-4,4',6,6'-tetrayl)tetraacrylate;
$\mathbf{L^{10b}}$ = *(R)*-2,2'-dihydroxy-1,1'-dinaphthyl-4,4',6,6'-tetrakis(4-benzoate);
$\mathbf{L^{11b}}$ = *(R)*- 4,4',4",4'"-(1*E*,1'*E*,1"*E*,1'"*E*)-2,2',2",2'"-(2,2'-dihydroxy-1,1'-binaphthyl-4,4',6,6'-tetrayl)tetrakis(ethene-2,1-diyl)tetrabenzoate;
$\mathbf{L^{12}}$ = (*R*,*R*)-(-)-*N*,*N*'-Bis(3-carboxyl-5-*tert*-butylsalicylidene)-1,2-cyclohexanediamino manganese (III) chloride;
$\mathbf{L^{13}}$ = (2*E*,2'*E*)-3,3'-(5,5'-(1*E*,1'*E*)-(1*R*,2*R*)-cyclohexane-1,2-diylbis(azan-1-yl-1-ylidene)bis(methan-1-yl-1-ylidene)bis(3-*tert*-butyl-4-hydroxy-5,1-phenylene))diacrylic acid manganese (III) chloride;
$\mathbf{NH_2BDC}$ = 2-amino-1,4-benzenedicarboxylate;
AD = Adenine;
ABDC = 4,4'-azobenzenedicarboxylate;
$\mathbf{NH_2}$**-TPDC** = 2'-amino-1,1':4,1"-terphenyl-4,4"-dicarboxylate;
SDC = 4,4'-stilbenedicarboxylate;
BTTB = 4,4',4"-(benzene-1,3,5-triyl-tris(oxy))tribenzoate;
DEF = *N*,*N*'-diethylformamide;
DMF = *N*,*N*'-dimethylformamide;
DMA = *N*,*N*'-dimethylacetamide;
NMP = *N*-methyl-2-pyrrolidinone;
DMSO = dimethyl sulfoxide;
NMF = *N*-methylformamide;
[b] Data from refs (for comparative analysis, all of the parameters are only worth reporting to one decimal place);
[c] Topological symbols from ref.;
[d] N.A. = Not Available;
[e] Data from ref. S14;
[f] Data from ref. S20.

Table S2 The adsorption information and thermal stability of reported mesoMOFs.

Publish Time	*meso*MOF Code	*meso*MOF Formula[a]	Structural Type	BET Surface Area ($m^2\ g^{-1}$)	Langmuir Surface Area ($m^2\ g^{-1}$)	Pore Volume ($cm^3\ g^{-1}$)	T_{max} of Thermal Stability[b]	Activated T_{max} for Sorption	Ref.
2004	MIL-100	$[Cr_3F(H_2O)_3O(\mathbf{BTC})_2](H_2O)_n$ ($n \approx 28$)	Cage	N.A.[c]	3100	1.16	~275 °C[b]	N.A.[c]	S1
2005 2006	MIL-101	$[Cr_3F(H_2O)_2O(\mathbf{BDC})_3](H_2O)_n$ ($n \approx 25$)	Cage	4100[d]	4500~5500[d] 4000/5500[e]	2.0[d]	~275 °C[b]	100 °C 200 °C	S2 S3
2007	N.A.[c]	$[(Tb_{16}(\mathbf{TATB})_{16}(DMA)_{24}](DMA)_{91}(H_2O)_{108}$	Cage	1419 /1783	2887 /3855	0.98 /1.29	~320 °C[b]	80 °C /160 °C	S4
2008	N.A.[c]	$[Cu_6O(\mathbf{TZI})_3(H_2O)_9(NO_3)](H_2O)_{15}$	Cage	2847	3223	1.01	N.A.[c]	85 °C	S5
2008	ZIF-95 ZIF-100	$[Zn(\mathbf{CBIM})_2]$ $[Zn_{20}(\mathbf{CBIM})_{39}(OH)]$	Cage	1050 595	1240 780	0.43 0.37	~500 °C[b]	100 °C	S6
2009	UMCM-2	$[Zn_4O(\mathbf{T^2DC})(\mathbf{BTB})_{4/3}]$	Cage	5200	6060	N.A.[c]	~400 °C[b]	300 °C	S7
2009	PCN-61 PCN-66	$[Cu_3(\mathbf{BTEI})(H_2O)_3](DMF)_5(H_2O)_4$ $[Cu_3(\mathbf{NTEI})(H_2O)_3](DMA)_{21}(H_2O)_{10}$	Cage	3000 4000	3500 4600	1.36 1.63	< 300°C[b] < 200°C[b]	150 °C 150 °C	S8
2009	MIL-101-NDC	$[Cr_3(OH)(H_2O)_2(\mu_3\text{-}O)(2,6\text{-}\mathbf{NDC})_3]$(guest) (guest = H_2O, EtOH)	Cage	2100[f] /1100[g]	N.A.[c]	N.A.[c]	~260 °C[b]	160 °C	S9
2009	NOTT-112	$[Cu_3(\mathbf{L^1})(H_2O)_3](DMSO)_8(DMF)_{15}(H_2O)_3$	Cage	3800	N.A.[c]	1.62[h] /1.69[i]	~350 °C[b]	115 °C	S10
2009	DUT-6	$[Zn_4O(2,6\text{-}\mathbf{NDC})(\mathbf{BTB})_{4/3}](DEF)_{16}(H_2O)_{9/2}$	Cage	N.A.[c]	N.A.[c]	2.02	380 °C	30 °C	S11
2010	MOF-180 MOF-200 MOF-210	$[Zn_4O(\mathbf{BTE})_2](DMF)_{14.8}(NMP)_{15.6}$ $[Zn_4O(\mathbf{BBC})_2(H_2O)_3](DEF)_{29.4}(NMP)_{33.2}$ $[Zn_4O(\mathbf{BTE})_{4/3}(\mathbf{BPDC})](DMF)_{25.7}(NMP)_{24.6}$	Cage	N.A.[c] 4530 6240	N.A.[c] 10400 10400	N.A.[c] 3.59 3.60	~350 °C[b] ~350 °C[b] ~360 °C[b]	N.A.[c] SCD[j], 40 °C SCD[j], 40 °C	S12

Table S2 (*continued*)

Publish Time	*meso*MOF Code	*meso*MOF Formula[a]	Structural Type	BET Surface Area ($m^2\ g^{-1}$)	Langmuir Surface Area ($m^2\ g^{-1}$)	Pore Volume ($cm^3\ g^{-1}$)	T_{max} of Thermal Stability[b]	Activated T_{max} for Sorption	Ref.
2010	NOTT-116	$[Cu_3(\mathbf{PTEI})(H_2O)_3](DMF)_{16}(H_2O)_{26}$	Cage	4664	N.A.[c]	2.17	~300 °C[b]	100 °C	S13
2010	PCN-68	$[Cu_3(\mathbf{PTEI})(H_2O)_3](DMF)_{33}(H_2O)_{13}$		5109	6033	2.13	~275 °C[b]	100 °C	S14
2010	PCN-610	$[Cu_3(\mathbf{TTEI})(H_2O)_3](DMF)_{22}(H_2O)_{19}$[e]	Cage	N.A.[c]	N.A.[c]	N.A.[c]	~320 °C[b]	N.A.[c]	S14
2010	NU-100	N.A.[c]		6143	N.A.[c]	2.82	~325 °C[b]	SCD[j], 110 °C	S15
2010	PCN-100	$[Zn_4O(\mathbf{TATAB})_2](DEF)_{17}(H_2O)_3$	Cage	N.A.[c]	860	0.58	~150 °C[b]	R.T.[k]	S16
	PCN-101	$[Zn_4O(\mathbf{BTATB})_2](DEF)_{16}(H_2O)_5$		N.A.[c]	1140	0.75	~180 °C[b]	R.T.[k]	
2010	N.A.[c]	$[(In_3O)(OH)(\mathbf{ADC})_2(\mathbf{IN})_2](H_2O)_{4.67}$	Cage	1857	1496	N.A.[c]	~350 °C[b]	100 °C	S17
2011	JT-1	$[\{Cu_7(OH)_2(\mathbf{L^2})_3\}\{Cu_6(OH)_2(SO_4)_3(S_3O_{10})_2\}](H_2O)_{10}$	Cage	375	N.A.[c]	N.A.[c]	~200 °C[b]	N.A.[c]	S18
	JT-2	$[\{Cu_7(OH)_2(\mathbf{L^2})_3\}_2\{Cu_6(OH)_2(SO_4)_6(S_2O_7)\}\{Cu_3(SO_4)(H_2O)_6\}](H_2O)_{18}$		421	N.A.[c]	N.A.[c]	~200 °C[b]	N.A.[c]	
2011	PCN-69	$[Cu_3(\mathbf{BTTI})(H_2O)_3](DMF)_{20}(H_2O)_{16}$	Cage	3989	6278	2.17	~280 °C[b]	100 °C	S19
2011	NOTT-119	$[Cu_3(\mathbf{BTTI})(H_2O)_3](DMF)_{35}(H_2O)_{35}$		4118	N.A.[c]	2.35	315 °C[b]	110 °C	S20
2011	N.A.[c]	$[Zn_4O(\mathbf{L^3})_{1.5}]$	Cage	N.A.[c]	N.A.[c]	N.A.[c]	~370 °C[b]	R.T.[k]	S21
		$[Zn_4O(\mathbf{L^4})_{1.5}]$					~380 °C[b]		
		$[Zn_4O(\mathbf{L^5})_{1.5}]$					~360 °C[b]		
2012	PCN-53	$[Fe_3O(H_2O)_3(\mathbf{BTTC})_2](DMF)_{10}$	Cage	2817	N.A.[c]	1.57	~200 °C[b]	120 °C	S22
2012	PCN-105	$[Cd_4Na(H_2O)_2(\mathbf{HTDBD})_3(\mathbf{TDBD})](DMF)_{10}(EtOH)_6(H_2O)_3$	Cage	1067	1317	N.A.[c]	~350 °C[b]	60 °C	S23
2012	DUT-25	$[Zn_4O(\mathbf{BENZTB})(\mathbf{BTB})_{2/3}](DEF)_{16}(H_2O)_{7/2}$	Cage	4670	N.A.[c]	2.22	~350 °C[b]	SCD[j], 30 °C	S24
2012	SUMOF-1-Zn	$[Zn_6(\mathbf{BTB})_4(4,4'\text{-}\mathbf{bpy})_3](solvent)_x$	Cage	N.A.[c]	N.A.[c]	N.A.[c]	~260 °C[b]	N.A.[c]	S25
	SUMOF-1-Co	$[Co_6(\mathbf{BTB})_4(4,4'\text{-}\mathbf{bpy})_3](solvent)_x$					~350 °C[b]		

Table S2 (*continued*)

Publish Time	*meso*MOF Code	*meso*MOF Formula[a]	Structural Type	BET Surface Area ($m^2\ g^{-1}$)	Langmuir Surface Area ($m^2\ g^{-1}$)	Pore Volume ($cm^3\ g^{-1}$)	T_{max} of Thermal Stability[b]	Activated T_{max} for Sorption	Ref.
2012	N.A.[c]	$[Cu_3(\mathbf{L^6})]$	Cage	3288	N.A.[c]	1.77	~125 °C[b]	100 °C	S26
		$[Cu_3(\mathbf{L^7})]$		3360	N.A.[c]	1.91	~125 °C[b]	100 °C	
2013	MIL-143	$[Fe_3O(Cl^-)(H_2O)_2(\mathbf{BDC})_{3/2}(\mathbf{BTB})](solvent)_n$	Cage	2150	N.A.[c]	1.18	~200 °C	100 °C	S27
2013	N.A.[c]	$[(CH_3)_2NH_2]_2[Zn(\mathbf{TATAT})_{2/3}](DMF)_3(H_2O)$	Cage	N.A.[c]	N.A.[c]	N.A.[c]	N.A.[c]	N.A.[c]	S28
2002	IRMOF-16	$[Zn_4O(\mathbf{TPDC})_3](DEF)_{17}(H_2O)_2$	3D Channel	N.A.[c]	N.A.[c]	N.A.[c]	N.A.[c]	N.A.[c]	S29
	IRMOF-14	$[Zn_4O(\mathbf{PDC})_3](DEF)_6(H_2O)_5$		N.A.[c]	1936	0.69		150 °C	
	IRMOF-12	$[Zn_4O(\mathbf{HPDC})_3](DEF)_{10}(H_2O)$		N.A.[c]	1750	0.61		150 °C	
	IRMOF-10	$[Zn_4O(\mathbf{BPDC})_3](DEF)_{12}(H_2O)$		N.A.[c]	N.A.[c]	N.A.[c]		N.A.[c]	
	IRMOF-8	$[Zn_4O(2,6\text{-}\mathbf{NDC})_3](DEF)_6$		N.A.[c]	N.A.[c]	N.A.[c]		N.A.[c]	
2006	mesoMOF-1	$[Cu_3(\mathbf{TATAB})_2(H_2O)_3](DMF)_8(H_2O)_9$	3D Channel	N.A.[c]	N.A.[c]	N.A.[c]	~180 °C[b]	80 °C	S30
2009	N.A.[c]	$[Cu_2(\mathbf{L^8})(H_2O)_2](DMF)_{14}(H_2O)_5$	3D Channel	1020	1127	N.A.[c]	~260 °C[b]	Freeze-Dried Method	S31
2010	CMOF-2a	$[(R\text{–}\mathbf{L^{9a}})Cu_2(H_2O)_2](DMF)_{15}(H_2O)_{11}$	3D Channel	0	N.A.[c]	N.A.[c]	~200 °C[b]	N.A.[c]	S32
	CMOF-3a	$[(R\text{–}\mathbf{L^{10a}})Cu_2(H_2O)_2](DEF)_{12}(H_2O)_{16}$		~240			~260 °C[b]		
	CMOF-4a	$[(R\text{–}\mathbf{L^{11a}})Cu_2(H_2O)_2](DEF)_{10}(DMA)_{14}(H_2O)_5$		0			~260 °C[b]		
	CMOF-2b	$[(R\text{–}\mathbf{L^{9b}})Cu_2(H_2O)_2](DEF)_{11}(H_2O)_3$		0			~200 °C[b]		
	CMOF-3b	$[(R\text{-}\mathbf{L^{10b}})Cu_2(H_2O)_2](DMF)_{13}(^i PrOH)_{11}(H_2O)_{4.5}$		0			~260 °C[b]		
	CMOF-4b	$[(R\text{–}\mathbf{L^{11b}})Cu_2(H_2O)_2](DEF)_{6.5}(DMF)_{19}(^i PrOH)_{8.5}(H_2O)_2$		0			~250 °C[b]		
2010	CMOF-2	$[Zn_4(\mu_4\text{-}O)(\mathbf{L^{12}})_3](DEF)_{22}(H_2O)_4$	3D Channel	N.A.[c]	N.A.[c]	N.A.[c]	~200 °C[b]	N.A.[c]	S33
	CMOF-3	$[Zn_4(\mu_4\text{-}O)(\mathbf{L^{13}})_3](DMF)_{42}$					~250 °C[b]		
	CMOF-4	$[Zn_4(\mu_4\text{-}O)(\mathbf{L^{13}})_3](DEF)_{37}(EtOH)_{23}(H_2O)_4$					~250 °C[b]		

Table S2 (*continued*)

Publish Time	*meso*MOF Code	*meso*MOF Formula[a]	Structural Type	BET Surface Area ($m^2\ g^{-1}$)	Langmuir Surface Area ($m^2\ g^{-1}$)	Pore Volume ($cm^3\ g^{-1}$)	T_{max} of Thermal Stability[b]	Activated T_{max} for Sorption	Ref.
2010	Cd-MOF	$[Cd(\mathbf{NH_2BDC})(4,4'\text{-}\mathbf{bpy})](DMF)_3(H_2O)_{4.5}$	3D Channel	N.A.[c]	N.A.[c]	N.A.[c]	~240 °C[b]	N.A.[c]	S34
2012	PCN-222(Fe)	N.A.[c]	3D Channel	2200	N.A.[c]	1.56	~370 °C[b]	120 °C	S35
2012	Bio-MOF-100	$[(CH_3)_2NH_2]_4[Zn_8(\mathbf{AD})_4(\mathbf{BPDC})_6O_2](DMF)_{49}(H_2O)_{31}$	3D Channel	4300	N.A.[c]	4.3	~350 °C[b]	SCD[j], 100 °C	S36
2013	N.A.[c]	$[(CH_3)_2NH_2]_2[ZnNa_2(\mu_2\text{-}H_2O)_2(H_2O)_2(\mathbf{TATAT})](DMF)_2$	3D Channel	N.A.[c]	N.A.[c]	N.A.[c]	~350 °C[b]	N.A.[c]	S28
2013	Bio-MOF-101	$[(CH_3)_2NH_2]_2[Zn_8(\mathbf{AD})_4(2,6\text{-}\mathbf{NDC})_6(OH)_2](DMF)_{34}(H_2O)_{13.4}$	3D Channel	4410	N.A.[c]	2.83	N.A.[c]	SCD[j], R.T.[k]	S37
	Bio-MOF-102	$[(CH_3)_2NH_2]_2[Zn_8(\mathbf{AD})_4(\mathbf{ABDC})_6(OH)_2]$		3222	N.A.[c]	4.36	N.A.[c]		
	Bio-MOF-103	$[(CH_3)_2NH_2]_2[Zn_8(\mathbf{AD})_4(\mathbf{NH_2}\text{-}\mathbf{TPDC})_6(OH)_2]$		2704	N.A.[c]	4.13	N.A.[c]		
2008	UMCM-1	$[Zn_4O(\mathbf{BDC})(\mathbf{BTB})_{4/3}]$	Microcage+ 1D Channel	4160	6500	N.A.[c]	~400 °C[b]	R.T.[k]	S38
2013	CYCU-3	[Al(OH)(**SDC**)]	Multiple 1D Channel	2757	3884	1.39	~300 °C[b]	150 °C	S39
2007	JUC-48	$[Cd_3(\mathbf{BPDC})_3(DMF)](DMF)_5(H_2O)_{18}$	1D Channel	629	880	0.19	~380 °C[b]	R.T.[k]	S40
2012	IRMOF-74-III	N.A.[c]	1D Channel	2440	3750	1.23	< 300 °C[b]	130 °C	S41
	IRMOF-74-IV			2480	5370	1.60			
	IRMOF-74-V			2230	6940	1.89			
	IRMOF-74-VI			1600	5880	1.65			
	IRMOF-74-VII			1800	8320	2.12			
	IRMOF-74-IX			1920	9410	2.51			
	IRMOF-74-XI			1760	9880	3.41			

Table S2 (*continued*)

Publish Time	*meso*MOF Code	*meso*MOF Formula[a]	Structural Type	BET Surface Area ($m^2 g^{-1}$)	Langmuir Surface Area ($m^2 g^{-1}$)	Pore Volume ($cm^3 g^{-1}$)	T_{max} of Thermal Stability[b]	Activated T_{max} for Sorption	Ref.
	437-MOF	**$[In(BTTB)_{2/3}(OH)](NMF)_5(H_2O)_4$**	**1D Channel**	**2379**	**N.A.[c]**	**1.11**	**Over 400°C[l]**	**360 °C**	**This work**

[a] Abbreviations: see the footnote of Table S1;
[b] Date from TGA curves;
[c] N.A. = Not Available;
[d] Data from ref. S2;
[e] Data from ref. S3;
[f] Based on the activated samples;
[g] Based on the as-synthesized samples;
[h] Data from N_2 isotherm;
[i] Data from Ar isotherm;
[j] SCD = Supercritical Carbon Dioxide;
[k] R.T. = Room Temperature;
[l] Data from the long-term heating treatment (at least 3h) under vacuum (< 10^{-3} Torr at least).

Table S3 Crystallographic data and structure refinement details for 437-MOFs.

	437-MOF	**437-MOF-CH_2Cl_2**	**437-MOF-boiling water**
Empirical formula	$C_{18}H_{11}O_7In$	$C_{18}H_{11}O_7In$	$C_{18}H_{11}O_7In$
Formula weight	454.09	454.09	454.09
Crystal system	Hexagonal	Hexagonal	Hexagonal
Space group	*P*6$_3$/*mcm*	*P*6$_3$/*mcm*	*P*6$_3$/*mcm*
Crystal size (mm^3)	0.28×0.10×0.09	0.22×0.11×0.10	0.24×0.12×0.10
a (Å)	32.3006(7)	32.182(2)	32.2297(13)
b (Å)	32.3006(7)	32.182(2)	32.2297(13)
c (Å)	7.2707(2)	7.2741(4)	7.2618(4)
Volume ($Å^3$)	6569.4(3)	6524.5(7)	6532.6(5)
Z	6	6	6
D (g cm^{-3})	0.689	0.693	0.693
μ (mm^{-1})	4.453	4.483	4.478
F (000)	1344	1344	1344
R_{int}	0.1070	0.0763	0.1032
Goodness-of-fit on F^2	1.138	1.299	1.039
$R_1{}^a$ / $wR_2{}^b$ [$I>2\sigma(I)$]	0.0936 / 0.1934	0.1676 / 0.4097	0.1063 / 0.2962
$R_1{}^a$ / $wR_2{}^b$ (all data)	0.1109 / 0.2003	0.2002 / 0.4309	0.1687 / 0.3410
CCDC number	952936	952937	952938

^{a} $R_1 = \Sigma||F_o| - |F_c||/\Sigma|F_o|$. ^{b} $wR_2 = |\Sigma w(|F_o|^2 - |F_c|^2)|/\Sigma|w(F_o)^2|^{1/2}$, where $w = 1/[\sigma^2(F_o^2) + (aP)^2 + bP]$. $P = (F_o^2 + 2F_c^2)/3$.

Table S4 Comparison of the selected bond lengths (Å) and angles (°) for 437-MOFs.[a]

	437-MOF	**437-MOF-CH_2Cl_2**	**437-MOF-boiling water**
In1–O1	2.167(5)	2.152(17)	2.153(5)
In1–O2	2.075(6)	2.115(13)	2.085(6)
O1–In1–O2	90.3(2)	89.9(5)	90.2(2)
O1–In1–O1$^{\#1}$	94.7(3)	97.7(10)	94.6(3)

[a] Symmetry code: #1 = $x - y + 1, -y + 2, z$.

Table S5 Structural features of the reported trigonal carboxylate ligands.[a]

Trigonal ligands	α, β, and γ (°)[a]		*Ref.*
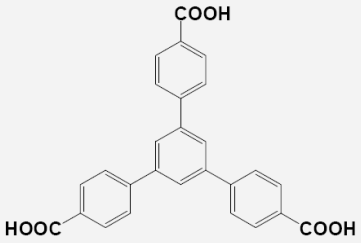 H_3BTB	(α_1, α_2, α_3):	**0~83.5°**	S7 S12 S24 S25 S38 S46–S88
	(β_1, β_2, β_3):	**0~81.3°**	
	(γ_1, γ_2, γ_3):	**118.7~123.9°**	
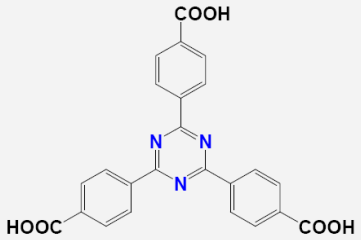 H_3TATB	(α_1, α_2, α_3):	**0.5~4.8°**	S89–S91
	(β_1, β_2, β_3):	**2.1~4.1°**	
	(γ_1, γ_2, γ_3):	**119.2~119.9°**	
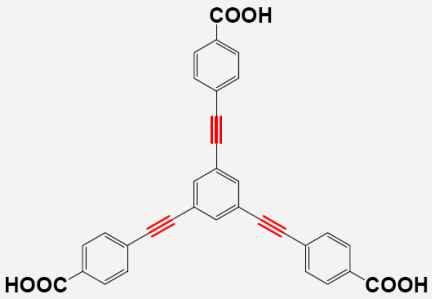 H_3BTE	(α_1, α_2, α_3):	**4.2~20.6°**	S12 S57 S92
	(β_1, β_2, β_3):	**12.6~22.6°**	
	(γ_1, γ_2, γ_3):	**110.6~123.1°**	
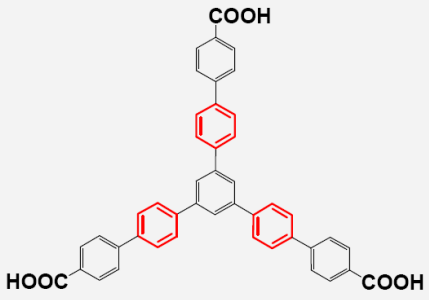 H_3BBC	(α_1, α_2, α_3):	**2.1~83.5°**	S12 S51 S93
	(β_1, β_2, β_3):	**4.9~81.3°**	
	(γ_1, γ_2, γ_3):	**111.9~123.9°**	

Trigonal ligands	α, β, and γ (°)[a]	Ref.
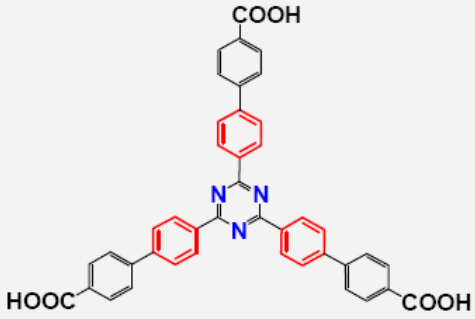 H$_3$TAPB	(α_1, α_2, α_3): **27.9~44.9°** (β_1, β_2, β_3): **29.4~39.2°** (γ_1, γ_2, γ_3): **118.9~121.7°**	S51
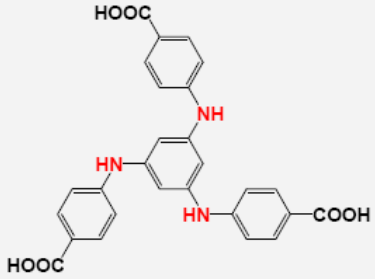 H$_3$BTATB	$\alpha_1 = \alpha_2 = \alpha_3 = 30.7°$ $\beta_1 = \beta_2 = \beta_3 = 36.5°$ (γ_1, γ_2, γ_3): **117.5~120.7°**	S16
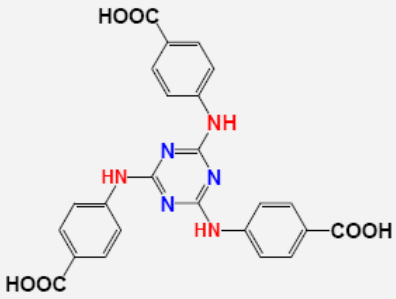 H$_3$TATAB	(α_1, α_2, α_3): **15.1~21.1°** (β_1, β_2, β_3): **19.5~25.6°** (γ_1, γ_2, γ_3): **119.5~119.9°**	S16 S30
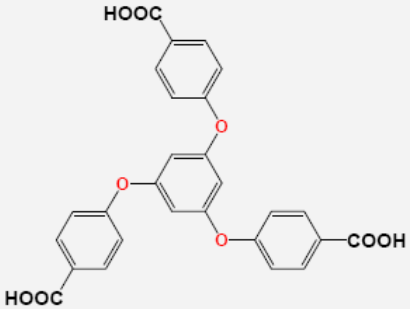 H$_3$BTTB	$\alpha_1 = \alpha_2 = \alpha_3 = 90°$ $\beta_1 = \beta_2 = \beta_3 = 90°$ $\gamma_1 = \gamma_2 = \gamma_3 = 120°$	**This work**

[a] For definitions of α, β, and γ, please refer to the captions for Fig. S6 and Fig. S7.

Table S6 Sorption parameters of 437-MOF samples from N_2 isotherms.

Sample	N_2 uptake (STP cm^3 g^{-1})[a]	BET surface area (m^2 g^{-1})[b]	Pore volume (cm^3 g^{-1})[c]
437-MOF-80	596	1576	0.92
437-MOF-240	646	1791	1.00
437-MOF-360	600	1533	0.93
437-MOF-boiling water	723	2379	1.11
437-MOF-boiling water-3h	576	1037	0.88

[a] The maximum uptake. [b] Calculated using N_2 adsorption data in the relative pressure ranging from 0.12 to 0.17. [c] Calculated by single point method from the amount of N_2 adsorb at maximum relative pressure.

Table S7 Sorption parameters of 437-MOF samples from Ar, O_2, and CO_2 isotherms.

Sample	Ar Uptake (STP cm^3 g^{-1})[a]	O_2 Uptake (STP cm^3 g^{-1})[a]	CO_2 Uptake (STP cm^3 g^{-1})[a]
437-MOF-80	704	728	421
437-MOF-240	734	722	454
437-MOF-360	684	690	359
437-MOF-boiling water	788	803	607
437-MOF-boiling water-3h	598	689	285

[a] The maximum uptake.

Table S8 The adsorption information and thermal stability of representative In(III)-based MOFs.

Publish Time	MOF Code	MOF Formula[a]	Pore Level	BET Surface Area ($m^2\ g^{-1}$)	Langmuir Surface Area ($m^2\ g^{-1}$)	Pore Volume ($cm^3\ g^{-1}$)	Accessible Void	T_{max} of Thermal Stability[b]	Activated T_{max} for Sorption	Ref.
2002	QMOF-2	$[InH(\mathbf{BDC})_2]$	Micro-	190	N.A.[c]	N.A.[c]	N.A.[c]	~270 °C[b]	N.A.[c]	S95
2006	Na^+-exchanged *rho*-ZMOF	$\|Na^+_{48}(H_2O)_{282}\|[In_{48}(\mathbf{HImDC})_{96}]$	Micro-	N.A.[c]	1067	N.A.[c]	N.A.[c]	N.A.[c]	105 °C	S96
2007	N.A.[c]	$[In_3O(\mathbf{L^1})_{1.5}(H_2O)_3](H_2O)_3(NO_3)$	Micro-	N.A.[c]	1417	0.50	57.2 %	N.A.[c]	N.A.[c]	S97
2008	*usf*-ZMOF	$[In_5(\mathbf{HImDC})_{10}](1,2\text{-}H_2\mathbf{DACH})_{2.5}(DMF)_3(CH_3CN)_2(H_2O)_{10}$	Micro-	N.A.[c]	520	0.20	50 %	~240 °C	N.A.[c]	S98
2008	N.A.[c]	$[In(OH)(\mathbf{HIPPB})]$	Micro-	215	N.A.[c]	N.A.[c]	18 %	~450 °C	250 °C	S99
2008	MIL-68(In)	$[In(OH)(\mathbf{BDC})]$	Micro-	746	1139	0.44	N.A.[c]	~350 °C	150 °C	S100
2008	ATF-1	$[(CH_3)_2NH_2][In(\mathbf{THB})_2](DMF)_x$	Micro-	N.A.[c]	360.3	0.126	50.2 %	~300 °C	150 °C	S101
2008	N.A.[c] N.A.[c]	$[(CH_3)_2NH_2][In(\mathbf{L^2})]$ $[Li^+][In(\mathbf{L^2})]$	Micro-	820 1024	N.A.[c]	0.326 0.419	~56 % N.A.[c]	~390 °C ~390 °C	180 °C 180 °C	S102
2008	*sod*-ZMOF	$[In(4,6\text{-}\mathbf{PmDC})_2Na_{0.36}K_{1.28}](NO_3)_{0.64}(H_2O)_{2.1}$	Micro-	N.A.[c]	616	0.245	46 %	N.A.[c]	R.T.[d]	S103
2009	MOC-2 MOC-3	$[In_8(\mathbf{HImDC})_{12}](DMF)_6$ $[NH_4][In_8(\mathbf{HImDC})_{12}]$ $[In_8(\mathbf{HImDC})_{11}(\mathbf{ImDC})]$	Micro-	N.A.[c]	1420 456	0.535 0.1733	56.1 % ~31 %	~320 °C ~320 °C	135 °C 135 °C	S104
2009	N.A.[c]	$(choline)_3[In_3(\mathbf{BTC})_4](DMF)_2$ $(Et_4N)_3[In_3(\mathbf{BTC})_4](DEF)$	Micro-	507.8 206.9	711.8 291.8	N.A.[c]	66.2 % N.A.[c]	<300°C ~380 °C	100 °C 200 °C	S105
2009	NOTT-200 NOTT-201	$[H_2\mathbf{PPZ}][In_2(\mathbf{L^3})_2](DMF)_{3.5}(H_2O)_5$ $[Li_{1.5}(H_3O)_{0.5}][In_2(\mathbf{L^3})_2](H_2O)_{11}$	Micro-	180 580	N.A.[c]	0.136 0.239	35 % 42 %	~400 °C ~400 °C	120 °C 120 °C	S106
2009	N.A.[c]	$[Et_2NH_2][In(2,6\text{-}\mathbf{NDC})_2](H_2O)_2(DEF)$	Micro-	891.2[e] 247[f]	1233.9[e]	0.50[e] 0.17[f]	48.1 %	~400 °C	120 °C	S107
2010	N.A.[c]	$[In_2(OH)_2(\mathbf{TBAPy})](guests)$	Micro-	1189	1475	0.639	54 %	~380 °C	150 °C	S108

Table S8 (*continued*)

Publish Time	MOF Code	MOF Formula[a]	Pore Level	BET Surface Area ($m^2\ g^{-1}$)	Langmuir Surface Area ($m^2\ g^{-1}$)	Pore Volume ($cm^3\ g^{-1}$)	Accessible Void	T_{max} of Thermal Stability[b]	Activated T_{max} for Sorption	Ref.
2010	**N.A.**[c]	$[(In_3O)(OH)(\mathbf{ADC})_2(\mathbf{IN})_2](H_2O)_{4.67}$	Meso-	1496	1857	**N.A.**[c]	68.2 %	~**350 °C**	**100 °C**	S17
2010	**ZSA-2**	$\lvert K_3(NO_3)_3(H_2O)_{2.5}(CH_3CN)_3\rvert$ $[In_4(1,2\text{-}\mathbf{DACH})_4(\mathbf{TzDC})_4]$	Micro-	395	**N.A.**[c]	0.19	34.2 %	~**300 °C**	**85 °C**	S109
2010	**CPM-5**	$[(CH_3)_2NH_2][In_3O(\mathbf{BTC})_2(H_2O)_3]_2$ $[In_3(\mathbf{BTC})_4](DMF)_7(H_2O)_{23}$	Micro-	580	733	0.258	47.9 %	~**320 °C**	**230 °C**	S110
	CPM-6	$[CH_3NH_3][In_3O(\mathbf{BTC})_2(H_2O)_3]_2$ $[In_3(\mathbf{BTC})_4]$(solvents)		596	931	**N.A.**[c]	**N.A.**[c]	**N.A.**[c]	**230 °C**	
2010	**JUC-77**	$[In(OH)(\mathbf{OBA})](DMF)$	Micro-	976	1066	**N.A.**[c]	**N.A.**[c]	~**350 °C**	**90 °C**	S111
2011	**CPM-13**	$[CH_3NH_3]$ $[In_3O(\mathbf{BBDC})_3(HCO_2)_{3/2}(H_2O)]_2$(solvent)	Micro-	904	1441	0.487	62.8 %	~**400 °C**	**200 °C**	S61
2011	**N.A.**[c]	$[In_2(OH)_2(\mathbf{OBA})_2](DMF)_2$	Micro-	354.1	518.5	**N.A.**[c]	47.7 %	**N.A.**[c]	**180 °C**	S112
2011	**NOTT-207**	$Li_{1.2}(H_3O)_{0.8}[In_2(\mathbf{L^4})_2](H_2O)_{14}$	Micro-	474	**N.A.**[c]	0.206	40 %	~**400 °C**	**120 °C**	S113
	NOTT-208	$[H_2\mathbf{PPZ}][In_2(\mathbf{L^5})_2](DMF)_4(H_2O)_{5.5}$		687		0.287	39 %	~**400 °C**	**120 °C**	
	NOTT-209	$Li_{1.4}(H_3O)_{0.6}[In_2(\mathbf{L^5})_2]$(acetone)$_4(H_2O)_{11}$		729		0.303	43 %	~**400 °C**	**120 °C**	
2011	**N.A.**[c]	$[InH(\text{D-}\mathbf{CAM})_2]$	Micro-	497	607	0.132	49.3 %	~**240 °C**	**80 °C**	S114
2012	**In-soc-MOF**	$[In_3O(\mathbf{ABTC})_{1.5}(H_2O)_3](H_2O)_3(NO_3)$	Micro-	970	1180	0.37	**N.A.**[c]	**N.A.**[c]	**N.A.**[c]	S115
2012	**JUC-120** **MIL-100(In)**	**N.A.**[c]	Meso-	1456	**N.A.**[c]	0.636	**N.A.**[c]	~**400 °C**	**150 °C**	S116
2012	**N.A.**[c]	$[(CH_3)_2NH_2][In(\mathbf{NH_2BDC})_2](DMF)(H_2O)$	Micro-	573	633	**N.A.**[c]	**N.A.**[c]	~**240 °C**	**80 °C**	S117
2012	**N.A.**[c]	$[(CH_3)_2NH_2]$ $[In(\mathbf{BPDC})_2](DMF)_4(H_2O)_2$	Micro-	638	717	0.32	45.1 %	~**320 °C**	**40 °C**	S118

Table S8 (*continued*)

Publish Time	MOF Code	MOF Formula[a]	Pore Level	BET Surface Area ($m^2 g^{-1}$)	Langmuir Surface Area ($m^2 g^{-1}$)	Pore Volume ($cm^3 g^{-1}$)	Accessible void	T*max.* of Thermal Stability[b]	Activated T_{max} for Sorption	*Ref.*
2012	**CPM-19-Nd**	$[In_3Nd_2O(OH)_3(\mathbf{BTB})_3(H_2O)_6](NO_3)$(solvent)	Micro-	272	370	0.133	72.8 %	~**200 °C**	**150 °C**	S70
	CPM-20	$[InCo_2(OH)(\mathbf{IN})_3(\mathbf{BDC})_{3/2}]$(solvent)		1009	1134	0.404	**N.A.**[c]	~**300 °C**	**260 °C**	
2012	**N.A.**[c]	$[(CH_3)_2NH_2][In(\mathbf{L^6})](DMA)_3(H_2O)_2$	Micro-	19.35[g]/8.12[h]	30.38[g]/19.45[h]	**N.A.**[c]	70.3 %	~**320 °C**	**40 °C/80 °C**	S119
		$[TMA][In(\mathbf{L^6})](H_2O)_{10.5}$		13.67	21.35		**N.A.**[c]		**80 °C**	
		$[TEA][In(\mathbf{L^6})](H_2O)_7$		5.81	13.63		**N.A.**[c]		**80 °C**	
		$[TPA][In(\mathbf{L^6})](H_2O)_{3.5}$		37.41	57.05		**N.A.**[c]		**80 °C**	
		$[TBA][In(\mathbf{L^6})](H_2O)_{2.5}$		325.65	477.77		**N.A.**[c]		**80 °C**	
		$[(CH_3)_2NH_2]_2[In_2(\mathbf{L^7})](DMA)_5(H_2O)_2$		83.39[g]/97.77[h]	794.80[g]/816.56[h]		65.7 %		**40 °C/80 °C**	
		$[TMA]_2[In_2(\mathbf{L^7})](H_2O)_{19}$		13.40	22.55		**N.A.**[c]		**80 °C**	
		$[TEA]_2[In_2(\mathbf{L^7})](H_2O)_{18}$		754.63	1099.46		**N.A.**[c]		**80 °C**	
		$[TPA]_2[In_2(\mathbf{L^7})](H_2O)_{13}$		36.26	54.17		**N.A.**[c]		**80 °C**	
		$[(CH_3)_2NH_2][TBA][In_2(\mathbf{L^7})](H_2O)_{15}$		120.76	181.45		**N.A.**[c]		**80 °C**	
	CPM-15-Mg	$[(CH_3)_2NH_2]_4[In_6(\mathbf{BTC})_{12}]_2[(Mg_3OH)_4(H_2O)_{36}][(In_2MgO)_4(\mathbf{BTC})_4(H_2O)_{12}](solvent)_x$		398	474	0.169	**N.A.**[c]	~**300 °C**	**260 °C**	
2012	**CPM-15-Co**	$[(CH_3)_2NH_2]_4[In_6(\mathbf{BTC})_{12}]_2[(Co_3OH)_4(H_2O)_{36}][(In_2CoO)_4(\mathbf{BTC})_4(H_2O)_{12}](solvent)_x$	Micro-	344	563	0.181	**N.A.**[c]	~**300 °C**	**260 °C**	S120
	CPM-15-Ni	$[(CH_3)_2NH_2]_4[In_6(\mathbf{BTC})_{12}]_2[(Ni_3OH)_4(H_2O)_{36}][(In_2NiO)_4(\mathbf{BTC})_4(H_2O)_{12}](solvent)_x$		263	356	0.128	**N.A.**[c]	~**300 °C**	**260 °C**	
2012	**N.A.**[c]	$[In_3O(\mathbf{BPDC})_3(HCOO)(H_2O)_{1.5}](DMF)_x$	Micro-	1244.4	1785.13	0.628	62.6 %	~**220 °C**	**60 °C**	S121
2012	**NOTT-202**	$[(CH_3)_2NH_2]_{1.75}[In(\mathbf{L^8}]_{1.75}(DMF)_{12}(H_2O)_{10}$	Micro-	2220	**N.A.**[c]	0.953	70 %	~**380 °C**	**100 °C**	S122

Table S8 (*continued*)

Publish Time	MOF Code	MOF Formula[a]	Pore Level	BET Surface Area ($m^2\ g^{-1}$)	Langmuir Surface Area ($m^2\ g^{-1}$)	Pore Volume ($cm^3\ g^{-1}$)	Accessible void	T*max.* of Thermal Stability[b]	Activated T_{max} for Sorption	*Ref.*
2012	**InOF-1**	$[In_2(OH)_2(\mathbf{BPTC})](H_2O)_6$	Micro-	1065	1093	0.37	48.9 %	**~350 °C**	**N.A.**[c]	S123
2012	**JUC-101**	$(In_3O)(\mathbf{TDCPB})(H_2O)_3(guest)_x$	Micro-	3742	4202	1.409	78.6 %	**~300 °C**	**80 °C**	S124
2013	**N.A.**[c]	$[(CH_3)_2NH_2]_2[In_2\mathbf{L^7}](DMF)_4(H_2O)_{16}$	Micro-	752	991	**N.A.**[c]	43.9 %	**~400 °C**	**80 °C**	S125
2013	**N.A.**[c]	$[(CH_3)_2NH_2][In_2\mathbf{L^7}](DMF)_9(H_2O)_5$	Micro-	1555	1707	0.62	65.1 %	**<300°C**	**SCD**[i]**+40 °C**	S126
	437-MOF	$\mathbf{[In(BTTB)_{2/3}(OH)](NMF)_5(H_2O)_4}$	**Meso-**	**2379**	**N.A.**[c]	**1.11**	**65.3 %**	**Over 400°C**[j]	**360 °C**	**This work**

[a] Abbreviations:
BDC = benzene-1,4-dicarboxylate;
H_3ImDC = 4,5-imidazoledicarboxylic acid;
L^1 = 3,3',5,5'-azobenzenetetracarboxylate;
1,2-H_2**DACH** = 1,2-diaminocyclohexane;
HIPPB = 4,4'-(hexafluoroisopropylidene)bis(benzoate);
THB = thiophene-2,5-dicarboxylate;
L^2 = biphenyl-3,3',5,5'-tetracarboxylate;
4,6-**PmDC** = 4,6-pyrimidicarboxylate;
choline = $[(CH_3)_3NCH_2CH_2OH]^+$;
BTC = 1,3,5-benzenetricarboxylate;
H_2**PPZ** = piperazinium;
L^3 = 1,1',4',1'',4'',1'''-quaterphenyl-3,5,3''',5'''-tetracarboxylate;
2,6-**NDC** = 2,6-naphthalenedicarboxylate;
TBAPy = 1,3,6,8-tetrakis(*p*-benzoic acid)pyrene;
ADC = azobenzene-4,4'-dicarboxylate;
IN = isonicotinate;
1,2-**PDA** = 1,2-propanediamine;
H_3TzDC = 1,2,3-triazole-4,5-dicarboxylic acid;
OBA = 4,4'-oxybis(benzoate);
BBDC = 4,4'-biphenyldicarboxylate;

L^4 = [2,7-(9,10-dihydrophenanthrenediyl)]diisophthalate;
L^5 = 1,1',4',1",4",1'",4'",1'"'-pentaphenyl-3,5,3'"',5'"'-tetracarboxylate;
D-**CAM** = D-(+)-camphoric acid
ABTC = 3,3',5,5'-azobenzenetetracarboxylate;
BTB = 4,4',4"-benzene-1,3,5-triyl-tribenzoate;
L^6 = 5-(3,5-dicarboxybenzyloxy)isophthalate;
L^7 = tetrakis[(3,5-dicarboxyphenoxy)methyl]methane;
NH_2BDC = 2-amino terephthalate;
BPDC = 4,4'-biphenyldicarboxylate;
L^8 = biphenyl-3,3',5,5'-tetra-(phenyl-4-carboxylate);
TDCPB = 1,3,5-tris(3,5-di(4-carboxy-phenyl-1-yl)phenyl-1-yl)benzene;
BPTC = biphenyl-3,3',5,5'-tetracarboxylate;
BTTB = 4,4',4"-benzene-1,3,5-triyltris(oxy)) tribenzoate
DEF = *N*,*N*'-diethylformamide;
DMF = *N*,*N*'-dimethylformamide;
DMA = *N*,*N*'-dimethylacetamide;
NMF = *N*-methylformamide;
[b] Date from TGA curves;
[c] N.A. = Not Available;
[d] R.T. = Room Temperature
[e] Data calculated from solvent-exchanged samples;
[f] Data calculated from activated samples;
[g] for activated samples at 40 °C;
[h] for activated samples at 80 °C;
[i] SCD = Supercritical Carbon Dioxide;
[j] Data from the heating treatment (at least 3h) under vacuum (< 10^{-3} Torr).

References

S1 G. Férey, C. Serre, C. Mellot-Draznieks, F. Millange, S. Surblé, J. Dutour and I. Margiolaki, *Angew. Chem. Int. Ed.*, 2004, **43**, 6296–6301.

S2 G. Férey, C. Mellot-Draznieks, C. Serre, F. Millange, J. Dutour, S. Surblé and I. Margiolaki, *Science*, 2005, **309**, 2040–2042.

S3 M. Latroche, S. Surblé, C. Serre, C. Mellot-Draznieks, P. L. Llewellyn, J.-H. Lee, J.-S. Chang, S. H. Jhungn and G. Férey, *Angew. Chem. Int. Ed*., 2006, **45**, 8227–8231.

S4 Y. K. Park, S. B. Choi, H. Kim, K. Kim, B.-H. Won, K. Choi, J.-S. Choi, W.-S. Ahn, N. Won, S. Kim, D. H. Jung, S.-H. Choi, G.-H. Kim, S.-S. Cha, Y. H. Jhon, J. K. Yang and J. Kim, *Angew. Chem. Int. Ed*., 2007, **46**, 8230–8233.

S5 F. Nouar, J. F. Eubank, T. Bousquet, L. Wojtas, M. J. Zaworotko and M. Eddaoudi, *J. Am. Chem. Soc*., 2008, **130**, 1833–1835.

S6 B. Wang, A. P. Côté, H. Furukawa, M. O′Keeffe and O. M. Yaghi, *Nature*, 2008, **453**, 207–211.

S7 K. Koh, A. G. Wong-Foy and A. J. Matzger, *J. Am. Chem. Soc*., 2009, **131**, 4184–4185.

S8 D. Zhao, D. Yuan, D. Sun and H.-C Zhou, *J. Am. Chem. Soc*., 2009, **131**, 9186–9188.

S9 A. Sonnauer, F. Hoffmann, M. Fröba, L. Kienle, V. Duppel, M. Thommes, C. Serre, G. Férey and N. Stock, *Angew. Chem. Int. Ed*., 2009, **48**, 3791–3794.

S10 Y. Yan, X. Lin, S. Yang, A. J. Blake, A. Dailly, N. R. Champness, P. Hubberstey and M. Schröder, *Chem. Commun*., 2009, 1025–1027.

S11 N. Klein, I. Senkovska, K. Gedrich, U. Stoeck, A. Henschel, U. Mueller and S. Kaskel, *Angew. Chem. Int. Ed.*, 2009, **48**, 9954–9957.

S12 H. Furukawa, N. Ko, Y. B. Go, N. Aratani, S. B. Choi, E. Choi, A. Ö. Yazaydin, R. Q. Snurr, M. O′Keeffe, J. Kim and O. M. Yaghi, *Science*, 2010, **329**, 424–428.

S13 Y. Yan, I. Telepeni, S. Yang, X. Lin, W. Kockelmann, A. Dailly, A. J. Blake, W. Lewis, G. S. Walker, D. R. Allan, S. A. Barnett, N. R. Champness and M. Schröder, *J. Am. Chem. Soc*., 2010, **132**, 4092–4094.

S14 D. Yuan, D. Zhao, D. Sun and H.-C. Zhou, *Angew. Chem. Int. Ed.*, 2010, **49**, 5357–5361.

S15 O. K. Farha, A. Ö. Yazaydın, I. Eryazici, C. D. Malliakas, B. G. Hauser, M. G. Kanatzidis, S. T. Nguyen, R. Q. Snurr and J. T. Hupp, *Nat. Chem.*, 2010, **2**, 944–948.

S16 Q.-R. Fang, D.-Q. Yuan J. Sculley, J.-R. Li, Z.-B. Han and H.-C. Zhou, *Inorg. Chem*. 2010, **49**, 11637–11642.

S17 X. Gu, Z.-H. Lu and Q. Xu, *Chem. Commun*., 2010, **46**, 7400–7402.

S18 X. Xi, Y. Fang, T. Dong and Y. Cui, *Angew. Chem. Int. Ed*., 2011, **50**, 1154–1158.

S19 D. Yuan, D. Zhao and H.-C. Zhou, *Inorg. Chem*., 2011, **50**, 10528–10530.

S20 Y. Yan, S. Yang, A. J. Blake, W. Lewis, E. Poirier, S. A. Barnett, N. R. Champness and M. Schröder, *Chem. Commun*., 2011, **47**, 9995–9997.

S21 Y.-Q. Lan, H.-L. Jiang, S.-L. Li and Q. Xu, *Adv. Mater.*, 2011, **23**, 5015–5020.

S22 D. Yuan, R. B. Getman, Z. Wei, R. Q. Snurr and H.-C. Zhou, *Chem. Commun*., 2012, **48**, 3297–3299.

S23 Q.-R. Fang, D.-Q. Yuan, J. Sculley, W.-G. Lu and H.-C. Zhou, *Chem. Commun*., 2012, **48**,

254–256.

S24 R. Grünker, V. Bon, A. Heerwig, N. Klein, P. Müller, U. Stoeck, I. A. Baburin, U. Mueller, I. Senkovska and S. Kaskel, *Chem. Eur. J*., 2012, **18**, 13299–13303.

S25 Q. Yao, J. Sun, K. Li, J. Su, M. V. Peskov and X. Zou, *Dalton Trans*., 2012, **41**, 3953–3955.

S26 B. Zheng, Z. Yang, J. Bai, Y. Li and S. Li, *Chem. Commun*., 2012, **48**, 7025–7027.

S27 H. Chevreau, T. Devic, F. Salles, G. Maurin, N. Stock and C. Serre, *Angew. Chem. Int. Ed*., 2013, **52**, 5056–5060.

S28 C.-Y. Sun, X.-L. Wang, C. Qin, J.-L. Jin, Z.-M. Su, P. Huang and K.-Z. Shao, *Chem. Eur. J*., 2013, **19**, 3639–3645.

S29 M. Eddaoudi, J. Kim, N. Rosi, D. Vodak, J. Wachter, M. O′Keeffe and O. M. Yaghi, *Science*, 2002, **295***,* 469–472.

S30 X.-S. Wang, S. Ma, D. Sun, S. Parkin and H.-C. Zhou, *J. Am. Chem. Soc*., 2006, **128**, 16474–16475.

S31 L. Ma, A. Jin, Z. Xie and W. Lin, *Angew. Chem. Int. Ed*., 2009, **48**, 9905–9908.

S32 L. Ma, J. M. Falkowski, C. Abney and W. Lin, *Nature Chem.*, 2010, **2**, 838–846.

S33 F. Song, C. Wang, J. M. Falkowski, L. Ma and W. Lin, *J. Am. Chem. Soc*., 2010, **132**, 15390–15398.

S34 H.-L. Jiang, Y. Tatsu, Z.-H. Lu and Q. Xu, *J. Am. Chem. Soc*., 2010, **132**, 5586–5587.

S35 D. Feng, Z.-Y. Gu, J.-R. Li, H.-L. Jiang, Z. Wei and H.-C. Zhou, *Angew. Chem. Int. Ed*., 2012, **51**, 10307–10310.

S36 J. An, O. K. Farha, J. T. Hupp, E. Pohl, J. I. Yeh and N. L. Rosi, *Nature Commun.*, 2012, **3**, 604.

S37 T. Li, M. T. Kozlowski, E. A. Doud, M. N. Blakely and N. L. Rosi, *J. Am. Chem. Soc.*, 2013, **135**, 11688–11691.

S38 K. Koh, A. G. Wong-Foy and A. J. Matzger, *Angew. Chem. Int. Ed*., 2008, **47**, 677–680.

S39 S.-H. Lo, C.-H. Chien, Y.-L, Lai, C.-C. Yang, J. J. Lee, D. S. Raja and C.-H. Lin, *J. Mater. Chem. A*, 2013, **1**, 324–329.

S40 Q.-R. Fang, G.-S. Zhu, Z. Jin, Y.-Y. Ji, J.-W. Ye, M. Xue, H. Yang, Y. Wang and S.-L. Qiu, *Angew. Chem. Int. Ed*., 2007, **46**, 6638–6642.

S41 H. Deng, S. Grunder, K. E. Cordova, C. Valente, H. Furukawa, M. Hmadeh, F. Gándara, A. C. Whalley, Z. Liu, S. Asahina, H. Kazumori, M. O′Keeffe, O. Terasaki, J. F. Stoddart and O. M. Yaghi, *Science*, 2012, **336**, 1018–1023.

S42 K. Matsumoto, T. Higashihara and M. Ueda, *Macromolecules*, 2008, **41**, 7560–7565.

S43 *CrysAlis CCD* and *CrysAlis RED*, version 1.171.35.21, Oxford Diffraction Ltd: Yarnton, Oxfordshire, U.K, 2008.

S44 (*a*) G. M. Sheldrick, *SHELXTL*, *version 6.10*, Bruker Analytical X-ray Systems: Madison, WI, 2001; (*b*) G. M. Sheldrick, *Acta Cryst.*, 2008, **A64**, 112–122.

S45 A. L. Spek, *J. Appl. Crystallogr.*, 2003, **36**, 7–13.

S46 H. K. Chae, D. Y. Siberio-Pérez, J. Kim, Y. Go, M. Eddaoudi, A. J. Matzger, M. O′Keeffe and O. M. Yaghi, *Nature*, 2004, **427**, 523–527.

S47 J. Kim, B. Chen, T. M. Reineke, H. Li, M. Eddaoudi, D. B. Moler, M. O′Keeffe and O. M. Yaghi, *J. Am. Chem. Soc.*, 2001, **123**, 8239–8247.

S48 B. Chen, M. Eddaoudi, S. T. Hyde, M. O′Keeffe and O. M. Yaghi, *Science*, 2001, **291**, 1021–1023.

S49 A. C. Sudik, A. R. Millward, N. W. Ockwig, A. P. Côté, J. Kim and O. M. Yaghi, *J. Am. Chem. Soc*., 2005, **127**, 7110–7118.

S50 T. Devic, C. Serre, N. Audebrand, J. Marrot and G. Férey, *J. Am. Chem. Soc*., 2005, **127**, 12788–12789.

S51 H. Furukawa, Y. B. Go, N. Ko, Y. K. Park, F. J. Uribe-Romo, J. Kim, M. O′Keeffe and O. M. Yaghi, *Inorg. Chem*., 2011, **50**, 9147–9152.

S52 M. Kim, J. A. Boissonnault, C. A. Allen, P. V. Dau and S. M. Cohen, *Dalton Trans*., 2012, **41**, 6277–6282.

S53 B. Mu, F. Li, Y. Huang and K. S. Walton, *J. Mater. Chem*., 2012, **22**, 10172–10178.

S54 P. V. Dau, K. K. Tanabe and S. M. Cohen, *Chem. Commun.*, 2012, **48**, 9370–9372.

S55 J. Yu, Y. Cui, C. Wu, Y. Yang, Z. Wang, M. O′Keeffe, B. Chen and G. Qian, *Angew. Chem. Int. Ed*., 2012, **51**, 10542–10545.

S56 D. Kim, X. Song, J. H. Yoon and M. S. Lah, *Cryst. Growth Des*., 2012, **12**, 4186–4193.

S57 S. Du, C. Hu, J. -C. Xiao, H. Tan and W. Liao, *Chem. Commun*., 2012, **48**, 9177–9179.

S58 H. Xiang, W.-Y. Gao, D.-C. Zhong, L. Jiang and T.-B. Lu, *CrystEngComm*, 2011, **13**, 5825–5832.

S59 P. Maniam and N. Stock, *Inorg. Chem*., 2011, **50**, 5085–5097.

S60 D. Han, F.-L. Jiang, M.-Y. Wu, L. Chen, Q.-H. Chen and M.-C. Hong, *Chem. Commun*., 2011, **47**, 9861–9863.

S61 S.-T. Zheng, J. J. Bu, T. Wu, C. Chou, P. Feng and X. Bu, *Angew. Chem. Int. Ed*., 2011, **50**, 8858–8862.

S62 M. Padmanaban, P. Müller, C. Lieder, K. Gedrich, R. Grünker, V. Bon, I. Senkovska, S. Baumgärtner, S. Opelt, S. Paasch, E. Brunner, F. Glorius, E. Klemm and S. Kaskel, *Chem. Commun.* 2011, **47**, 12089–12091.

S63 M. L. Foo, S. Horike and S. Kitagawa, *Inorg. Chem*., 2011, **50**, 11853–11855.

S64 Y. D. Lampeka, L. V. Tsymbal, A. V. Barna, Y. L. Shuĺga, S. Shova and V. B. Arion, *Dalton Trans*., 2012, **41**, 4118–4125.

S65 Q. Lin, T. Wu, X. Bu and P. Feng, *Dalton Trans*., 2012, **41**, 3620–3622.

S66 D. F. Sava, L. E. S. Rohwer, M. A. Rodriguez and T. M. Nenoff, *J. Am. Chem. Soc.*, 2012, **134**, 3983–3986.

S67 N. Klein, I. Senkovska, I. A. Baburin, R. Grünker, U. Stoeck, M. Schlichtenmayer, B. Streppel, U. Mueller, S. Leoni, M. Hirscher and S. Kaskel, *Chem. Eur. J.*, 2011, **17**, 13007–13016.

S68 Z. Lin, R. Zou, J. Liang, W. Xia, D. Xia, Y. Wang, J. Lin, T. Hu, Q. Chen, X. Wang, Y. Zhao and A. K. Burrell, *J. Mater. Chem.*, 2012, **22**, 7813–7818.

S69 T. Dröge, A. Notzon, R. Fröhlich and F. Glorius, *Chem. Eur. J.*, 2011, **17**, 11974–11977.

S70 S.-T. Zheng, T. Wu, C. Chou, A. Fuhr, P. Feng and X. Bu, *J. Am. Chem. Soc.*, 2012, **134**, 4517–4520.

S71 M. Liu, W. Liao, C. Hu, S. Du and H. Zhang, *Angew. Chem. Int. Ed*., 2012, **51**, 1585–1588.

S72 R. Zou, A. I. Abdel-Fattah, H. Xu, A. K. Burrell, T. E. Larson, T. M. McCleskey, Q. Wei, M. T. Janicke, D. D. Hickmott, T. V. Timofeeva and Y. Zhao, *Cryst. Growth Des*., 2010, **10**, 1301–1306.

S73 J. Zhang, J. T. Bu, S. Chen, T. Wu, S. Zheng, Y. Chen, R. A. Nieto, P. Feng and X. Bu, *Angew. Chem. Int. Ed*., 2010, **49**, 8876–8879.

S74 B. Mu, Y. Huang and K. S. Walton, *CrystEngComm*, 2010, **12**, 2347–2349.

S75 I. A. Ibarra, X. Lin, S. Yang, A. J. Blake, G. S. Walker, S. A. Barnett, D. R. Allan, N. R. Champness, P. Hubberstey and M. Schröder, *Chem. Eur. J.*, 2010, **16**, 13671–13679.

S76 K. Gedrich, I. Senkovska, N. Klein, U. Stoeck, A. Henschel, M. R. Lohe, I. A. Baburin, U. Mueller and S. Kaskel, *Angew. Chem. Int. Ed.*, 2010, **49**, 8489–8492.

S77 D. Dang, P. Wu, C. He, Z. Xie and C. Duan, *J. Am. Chem. Soc.*, 2010, **132**, 14321–14323.

S78 B. Mu, F. Li and K. S. Walton, *Chem. Commun*., 2009, 2493–2495.

S79 L. Hou, J.-P. Zhang and X.-M. Chen, *Cryst. Growth Des*., 2009, **9**, 2415–2419.

S80 K. Sumida, M. R. Hill, S. Horike, A. Dailly and J. R. Long, *J. Am. Chem. Soc.*, 2009, **131**, 15120–15121.

S81 A. Company, N. Roques, M. Güell, V. Mugnaini, L. Gómez, I. Imaz, A. Datcu, M. Solà, J. M. Luis, J. Veciana, X. Ribas and M. Costas, *Dalton Trans*., 2008, 1679–1682.

S82 S. R. Caskey and A. J. Matzger, *Inorg. Chem*., 2008, **47**, 7942–7944.

S83 L. Hou, J.-P. Zhang, X.-M. Chen and S. W. Ng, *Chem. Commun*., 2008, 4019–4021.

S84 R. Heck, J. Bacsa, J. E. Warren, M. J. Rosseinsky and D. Bradshaw, *CrystEngComm*, 2008, **10**, 1687–1692.

S85 C. Volkringer, T. Loiseau, J. Marrot and G. Férey, *CrystEngComm*, 2009, **11**, 58–60.

S86 Z. Wang, K. K. Tanabe and S. M. Cohen, *Inorg. Chem*., 2009, **48**, 296–306.

S87 S. R. Caskey, A. G. Wong-Foy and A. J. Matzger, *Inorg. Chem*., 2008, **47**, 7751–7756.

S88 S. B. Choi, M. J. Seo, M. Cho, Y. Kim, M. K. Jin, D.-Y. Jung, J.-S. Choi, W.-S. Ahn, J. L. C. Rowsell and J. Kim, *Cryst. Growth Des*., 2007, **7**, 2290–2293.

S89 D. Sun, S. Ma, Y. Ke, T. M. Petersen and H.-C. Zhou, *Chem. Commun*., 2005, 2663–2665.

S90 D. Sun, S. Ma, Y. Ke, D. J. Collins and H.-C. Zhou, *J. Am. Chem. Soc*., 2006, **128**, 3896–3897.

S91 S. Ma, D. Yuan, X.-S. Wang and H.-C. Zhou, *Inorg. Chem*., 2009, **48**, 2072–2077.

S92 M. P. Suh, H. J. Choi, S. M. So and B. M. Kim, *Inorg. Chem.*, 2003, **42**, 676–678.

S93 D. Sun, Y. Ke, T. M. Mattox, S. Parkin and H.-C. Zhou, *Inorg. Chem*., 2006, **45**, 7566–7568.

S94 K. S. Walton and R. Q. Snurr, *J. Am. Chem. Soc.*, 2007, **129**, 8552–8556.

S95 J. Sun, L. Weng, Y. Zhou, J. Chen, Z. Chen, Z. Liu and D. Zhao, *Angew. Chem. Int. Ed.*, 2002, **41**, 4471–4473.

S96 Y. Liu, V. C. Kravtsov, R. Larsen and M. Eddaoudi, *Chem. Commun.*, 2006, 1488–1490.

S97 Y. Liu, J. F. Eubank, A. J. Cairns, J. Eckert, V. C. Kravtsov, R. Luebke and M. Eddaoudi, *Angew. Chem. Int. Ed.*, 2007, **46**, 3278–3283.

S98 Y. Liu, V. C. Kravtsov and M. Eddaoudi, *Angew. Chem. Int. Ed.*, 2008, **47**, 8446–8449.

S99 F. Gándara, B. Gomez-Lor, E. Gutiérrez-Puebla, M. Iglesias, M. A. Monge, D. M. Proserpio and N. Snejko, *Chem. Mater.*, 2008, **20**, 72–76.

S100 C. Volkringer, M. Meddouri, T. Loiseau, N. Guillou, J. Marrot, G. Férey, M. Haouas, F. Taulelle, N. Audebrand and M. Latroche, *Inorg. Chem.*, 2008, **47**, 11892–11901.

S101 J. Zhang, S. Chen, T. Wu, P. Feng and X. Bu, *J. Am. Chem. Soc.*, 2008, **130**, 12882–12883.

S102 S. Yang, X. Lin, A. J. Blake, K. M. Thomas, P. Hubberstey, N. R. Champness and M. Schröder, *Chem. Commun.*, 2008, 6108–6110.

S103 D. F. Sava, V. C. Kravtsov, F. Nouar, L. Wojtas, J. F. Eubank and M. Eddaoudi, *J. Am. Chem. Soc.*,

2008, **130**, 3768–3770.

S104 D. F. Sava, V. C. Kravtsov, J. Eckert, J. F. Eubank, F. Nouar and M. Eddaoudi, *J. Am. Chem. Soc.*, 2009, **131**, 10394–10396.

S105 S. Chen, J. Zhang, T. Wu, P. Feng and X. Bu, *J. Am. Chem. Soc.*, 2009, **131**, 16027–16029.

S106 S. Yang, X. Lin, A. J. Blake, G. S. Walker, P. Hubberstey, N. R. Champness and M. Schröder, *Nat. Chem.*, 2009, **1**, 487–493.

S107 S. Huh, T.-H. Kwon, N. Park, S.-J. Kim and Y. Kim, *Chem. Commun.*, 2009, 4953–4955.

S108 K. C. Stylianou, R. Heck, S. Y. Chong, J. Bacsa, J. T. A. Jones, Y. Z. Khimyak, D. Bradshaw and M. J. Rosseinsky, *J. Am. Chem. Soc.*, 2010, **132**, 4119–4130.

S109 S. Wang, T. Zhao, G. Li, L. Wojtas, Q. Huo, M. Eddaoudi and Y. Liu, *J. Am. Chem. Soc.*, 2010, **132**, 18038–18041.

S110 S.-T. Zheng, J. T. Bu, Y. Li, T. Wu, F. Zuo, P. Feng and X. Bu, *J. Am. Chem. Soc.*, 2010, **132**, 17062–17064.

S111 Z. Jin, H.-Y. Zhao, X.-J. Zhao, Q.-R. Fang, J. R. Long and G.-S. Zhu, *Chem. Commun.*, 2010, **46**, 8612–8614.

S112 Y.-X. Tan, F. Wang, Y. Kang and J. Zhang, *Chem. Commun.*, 2011, **47**, 770–772.

S113 S. Yang, G. S. B. Martin, J. J. Titman, A. J. Blake, D. R. Allan, N. R. Champness and M. Schröder, *Inorg. Chem.*, 2011, **50**, 9374–9384.

S114 L. Wang, T. Song, L. Huang, J. Xu, C. Li, C. Ji, L. Shan and L. Wang, *CrystEngComm*, 2011, **13**, 4005–4009.

S115 M. Pang, A. J. Cairns, Y. Liu, Y. Belmabkhout, H. C. Zeng and M. Eddaoudi, *J. Am. Chem. Soc.*, 2012, **134**, 13176–13179.

S116 F. Zhang, X. Zou, W. Feng, X. Zhao, X. Jing, F. Sun, H. Ren and G. Zhu, *J. Mater. Chem.*, 2012, **22**, 25019–25026.

S117 B. Yuan, D. Ma, X. Wang, Z. Li, Y. Li, H. Liu and D. He, *Chem. Commun.*, 2012, **48**, 1135–1137.

S118 J.-M. Gu, S.-J. Kim, Y. Kim and S. Huh, *CrystEngComm*, 2012, **14**, 1819–1824.

S119 Z.-J. Lin, T.-F. Liu, Y.-B. Huang, J. Lü and R. Cao, *Chem. Eur. J.*, 2012, **18**, 7896–7902.

S120 S.-T. Zheng, T. Wu, F. Zuo, C. Chou, P. Feng and X. Bu, *J. Am. Chem. Soc.*, 2012, **134**, 1934–1937.

S121 H. Yang, F. Wang, Y. Kang, T.-H. Li and J. Zhang, *Dalton Trans.*, 2012, **41**, 2873–2876.

S122 S. Yang, X. Lin, W. Lewis, M. Suyetin, E. Bichoutskaia, J. E. Parker, C. C. Tang, D. R. Allan, P. J. Rizkallah, P. Hubberstey, N. R. Champness, K. M. Thomas, A. J. Blake and M. Schröder, *Nature Mater.*, 2012, **11**, 710–716.

S123 J. Qian, F. Jiang, D. Yuan, M. Wu, S. Zhang, L. Zhang and M. Hong, *Chem. Commun.*, 2012, **48**, 9696–9698.

S124 J. Jia, F. Sun, T. Borjigin, H. Ren, T. Zhang, Z. Bian, L. Gao and G. Zhu, *Chem. Commun.*, 2012, **48**, 6010–6012.

S125 Y.-S. Xue, Y. He, L. Zhou, F.-J. Chen, Y. Xu, H.-B. Du, X.-Z. You and B. Chen, *J. Mater. Chem. A*, 2013, **1**, 4525–4530.

S126 Z.-J. Lin, Y.-B. Huang, T.-F. Liu, X.-Y. Li and R. Cao, *Inorg. Chem.*, 2013, **52**, 3127–3132.